doi:10.1093/brain/awr159 Brain 2011: 134; 2610–2626 | 2610

BRAIN
A JOURNAL OF NEUROLOGY

Pathological hallmarks of amyotrophic lateral sclerosis/frontotemporal lobar degeneration in transgenic mice produced with TDP-43 genomic fragments

Vivek Swarup,[1] Daniel Phaneuf,[1] Christine Bareil,[1] Janice Robertson,[2] Guy A. Rouleau,[3] Jasna Kriz[1] and Jean-Pierre Julien[1]

1 Centre de Recherche du Centre Hospitalier Universitaire de Québec, Department of Psychiatry and Neuroscience of Laval University, Québec, QC G1V 4G2, Canada
2 Department of Laboratory Medicine and Pathobiology, Centre for Research in Neurodegenerative Diseases, University of Toronto, Tanz Neuroscience Building, Toronto, ON M5S 3H2, Canada
3 Ste-Justine Hospital Research Center and Department of Medicine, University of Montreal, 3175 Cote Ste-Catherine, Montreal, Quebec H3T 1C5, Canada

Correspondence to: Dr Jean-Pierre Julien,
Centre de Recherche du Centre Hospitalier Universitaire de Québec,
Pavillon CHUL,
2705 Boulevard Laurier,
Quebec,
QC G1V 4G2, Canada
E-mail: jean-pierre.julien@crchul.ulaval.ca

Correspondence may also be addressed to: Dr Jasna Kriz. E-mail: jasna.kriz@crchul.ulaval.ca

Transactive response DNA-binding protein 43 ubiquitinated inclusions are a hallmark of amyotrophic lateral sclerosis and of frontotemporal lobar degeneration with ubiquitin-positive inclusions. Yet, mutations in *TARDBP*, the gene encoding these inclusions are associated with only 3% of sporadic and familial amyotrophic lateral sclerosis. Recent transgenic mouse studies have revealed a high degree of toxicity due to transactive response DNA-binding protein 43 proteins when overexpressed under the control of strong neuronal gene promoters, resulting in early paralysis and death, but without the presence of amyotrophic lateral sclerosis-like ubiquitinated transactive response DNA-binding protein 43-positive inclusions. To better mimic human amyotrophic lateral sclerosis, we generated transgenic mice that exhibit moderate and ubiquitous expression of transactive response DNA-binding protein 43 species using genomic fragments that encode wild-type human transactive response DNA-binding protein 43 or familial amyotrophic lateral sclerosis-linked mutant transactive response DNA-binding protein 43 (G348C) and (A315T). These novel transgenic mice develop many age-related pathological and biochemical changes reminiscent of human amyotrophic lateral sclerosis including ubiquitinated transactive response DNA-binding protein 43-positive inclusions, transactive response DNA-binding protein 43 cleavage fragments, intermediate filament abnormalities, axonopathy and neuroinflammation. All three transgenic mouse models (wild-type, G348C and A315T) exhibited impaired learning and memory capabilities during ageing, as well as motor dysfunction. Real-time imaging with the use of biophotonic transactive response DNA-binding protein 43 transgenic mice carrying a glial fibrillary acidic protein-luciferase reporter revealed that the behavioural defects were preceded by induction of astrogliosis, a finding consistent with a role for reactive astrocytes in amyotrophic lateral sclerosis pathogenesis. These novel transactive response DNA-binding protein 43 transgenic mice mimic several characteristics

Received January 26, 2011. Revised June 2, 2011. Accepted June 5, 2011. Advance Access publication July 13, 2011

of human amyotrophic lateral sclerosis-frontotemporal lobar degeneration and they should provide valuable animal models for testing therapeutic approaches.

Keywords: amyotrophic lateral sclerosis; motor neuron; neurodegeneration; TDP-43; inclusions

Abbreviations: FTLD-U = frontotemporal lobar degeneration with ubiquitin inclusions; GFAP = glial fibrillary acidic protein; luc = luciferase; PCR = polymerase chain reaction; TDP-43 = transactive response DNA-binding protein 43

Introduction

Amyotrophic lateral sclerosis is an adult-onset neurological disorder that is characterized by the selective loss of motor neurons leading to progressive weakness and muscle atrophy with eventual paralysis and death within 5 years of clinical onset. Frontotemporal lobar degeneration with ubiquitin inclusions (FTLD-U) is a relatively common cause of dementia among patients with onset before the age of 65, typically manifesting with behavioural changes or language impairment due to degeneration of subpopulations of cortical neurons in the frontal, temporal and insular regions (Seeley, 2008). Interestingly, 50% of patients with amyotrophic lateral sclerosis develop varying degrees of cognitive impairment (Lomen-Hoerth *et al.*, 2003), and ~15% of patients with FLTD-U also develop amyotrophic lateral sclerosis (Hodges *et al.*, 2004) and these two diseases co-segregate in some families (Talbot and Ansorge, 2006). The discovery that transactive response DNA-binding protein 43 (TDP-43) is present in cytoplasmic aggregates both in amyotrophic lateral sclerosis and FTLD-U provided the first conclusive molecular evidence that the two disorders share a common underlying mechanism (Neumann *et al.*, 2006).

Identified first as a regulator of HIV gene expression (Ou *et al.*, 1995), TDP-43 is a DNA/RNA-binding (Buratti *et al.*, 2001) protein that contains an N-terminal domain, two RNA-recognition motifs and a glycine-rich C-terminal domain thought to be important for mediating protein–protein interactions (Forman *et al.*, 2007; Lagier-Tourenne and Cleveland, 2009). Although TDP-43 has been implicated as a key factor regulating RNA splicing of human cystic fibrosis transmembrane conductance regulator (Buratti *et al.*, 2001), apolipoprotein A-II (Mercado *et al.*, 2005) and survival motor neuron protein (Bose *et al.*, 2008), the concept that TDP-43 can play a direct role in neurodegeneration was strengthened by recent reports that dominantly inherited missense mutations in TDP-43 are found in patients with familial amyotrophic lateral sclerosis (Gitcho *et al.*, 2008; Kabashi *et al.*, 2008; Rutherford *et al.*, 2008; Sreedharan *et al.*, 2008; Van Deerlin *et al.*, 2008; Yokoseki *et al.*, 2008). Mutations in TDP-43 are associated with the amyotrophic lateral sclerosis cluster in the C-terminal glycine-rich region, which is involved in protein–protein interactions between TDP-43 and other heterogeneous nuclear ribonuclear proteins (Lagier-Tourenne and Cleveland, 2009). The two TDP-43 mutations used in this study, A315T and G348C, have previously been reported (Gitcho *et al.*, 2008; Kabashi *et al.*, 2008). In neurodegenerative diseases, TDP-43 can be found in cytoplasmic ubiquitinated inclusions, where the protein is poorly soluble, hyperphosphorylated and cleaved into small fragments, making TDP-43 aggregates a hallmark pathology of amyotrophic lateral sclerosis and FTLD-U cases (Neumann *et al.*, 2006). Many of the transgenic mouse lines expressing wild-type or mutant TDP-43 reported to date have exhibited early paralysis followed by death (Wegorzewska *et al.*, 2009; Stallings *et al.*, 2010; Wils *et al.*, 2010). The available TDP-43 transgenic mouse models are based on high-level neuronal expression of TDP-43 transgenes. Transgenic mice expressing either wild-type or mutant TDP-43 (A315T and M337V) showed aggressive paralysis accompanied by increased ubiquitination (Stallings *et al.*, 2010; Wegorzewska *et al.*, 2009; Wils *et al.*, 2010; Xu *et al.*, 2010) but the lack of ubiquitinated TDP-43 inclusions raises concerns about their validity as models of human amyotrophic lateral sclerosis (Wegorzewska *et al.*, 2009). Another concern is the restricted expression of TDP-43 species with the use of Thy1.2 and prion promoters.

To better mimic the ubiquitous and moderate levels of TDP-43 occurring in the human context, we describe here the generation of new transgenic mouse models of amyotrophic lateral sclerosis/FTLD based on the expression of genomic TDP-43 fragments resulting in moderate and ubiquitous expression of wild-type and mutant TDP-43 species (A315T and G348C).

Materials and methods

DNA constructs and generation of wild-type, A315T and G348C TDP-43 transgenic mice

TARDBP (NM_007375) was amplified by polymerase chain reaction (PCR) from a human bacterial artificial chromosome clone (clone RPCI-11, number 829B14) along with the endogenous promoter (~4 kb). A315T and G348C mutations in TDP-43 were inserted using site-directed mutagenesis (Supplementary Fig. 1). The full-length genomic *TARDBP* (wild-type TDP-43, TDP-43^{A315T} and TDP-43^{G348C}) was linearized by Swa1 restriction enzyme and an 18-kb DNA fragment microinjected into 1-day-old mouse embryos (having a background of C3H X C57Bl/6). Founders were identified by Southern blotting (Supplementary Fig. 1) and were bred with non-transgenic C57Bl/6 mice to establish stable transgenic lines. The transgenic mice were identified by PCR amplification of the human *TARDBP* gene using the primer pairs listed in Table 1. The messenger RNA was analysed in brain and spinal cord by real-time PCR and protein analysed by western blot using monoclonal human TDP-43 antibody (Clone E2-D3, Abnova). To avoid the effects of genetic background, all experiments were performed on age-matched littermates. The use and maintenance of the mice described in this article were performed

Table 1 Primers for genotyping transgenic mice

Gene symbol	Forward primer	Reverse primer
Wild-type TDP-43	CTCTTTGTGGAGAGGAC	CCCCAACTGCTCTGTAG
TDP-43^{A315T}	CTCTTTGTGGAGAGGAC	TTATTACCCGATGGGCA
TDP-43^{G348C}	CTCTTTGTGGAGAGGAC	GGATTAATGCTGAACGT
GFAP-luc	GAAATGTCCGTTCGGTTGGCAGAAGC	CCAAAACCGTGATGGAATGGAACAACA

in accordance to the Guide of Care and Use of Experimental Animals of the Canadian Council on Animal Care.

Co-immunoprecipitation and western blot assays

Snap-frozen spinal cords of mice were harvested with lysis buffer containing 25 mM HEPES–NaOH (pH 7.9), 150 mM NaCl, 1.5 mM $MgCl_2$, 0.2 mM ethylenediaminetetraacetic acid, 0.5% Triton-X100, 1 mM dithiothreitol and protease inhibitor cocktail. Protein samples were estimated using the Bradford method. The lysate was incubated with 50 µl of Dynabeads (Protein-G beads, Invitrogen), anti-TDP-43 polyclonal (ProteinTech) or anti-peripherin polyclonal antibody (AB1530, Chemicon). After subsequent washing, the beads were incubated overnight at 4°C with 400 µg of tissue lysate. Antibody-bound complexes were eluted by boiling in Laemmli sample buffer. Supernatants were resolved by 10% sodium dodecyl sulphate polyacrylamide gel electrophoresis and transferred onto nitrocellulose membrane (Biorad). The membrane was incubated with anti-ubiquitin antibody (1:1000, Abcam). For other western blot assays, blots were incubated with primary antibodies against human monoclonal transactive response DNA-binding protein antibody (1:1000, Abnova, clone E2-D3), peripherin polyclonal antibody (1:1000, Chemcion, AB1530), peripherin monoclonal antibody (1:500, Chemicon, AB1527), Clone NR4 for light molecular weight neurofilament protein (1:1000, Sigma), Clone NN18 for medium molecular weight neurofilament protein (1:1000, Millipore) and Clone N52 for heavy molecular weight neurofilament protein (1:1000, Millipore). Immunoreactive proteins were then visualized by chemiluminescence (Perkin and Elmer) as described previously (Dequen *et al.*, 2008). Actin (1:10000, Chemicon) was used as a loading control.

Immunohistochemistry/ immunofluorescence microscopy

Paraformaldehyde (4%) fixed spinal cord and brain sections of mice were sectioned and fixed on slides. For immunohistochemistry, tissues were treated with hydrogen peroxide solution before permeabilization. After blocking with 5% normal goat serum for 1 h at room temperature, primary antibody incubations were performed in 1% normal goat serum in phosphate buffered solution with Tween-20 overnight, followed by an appropriate Alexa Fluor 488 or 594 secondary antibody (1:500, Invitrogen) for 1 h at room temperature. For immunohistochemistry, tissues were incubated in biotinylated secondary antibodies (1:500, Vector Labs), incubated in avidin–biotin complex and developed using DAB Kit (Vector labs). *Z*-stacked sections were viewed using ×40 or ×60 oil immersion objectives on an Olympus Fluoview™ Confocal System (Olympus).

Neurofilament enzyme-linked immunosorbent assay

Wells of microtitre plates were coated with 0.1% NaN_3/Tris-buffered saline including the primary antibodies (NR4; 1:600, N52; 1:1000, NN18; 1:500). The coated wells were incubated with 10% normal goat serum/0.2% Tween 20/Tris-buffered saline for 30 min at 37°C. After washing twice with Tris-buffered saline, an aliquot (100 µl) of the diluted samples was placed in each well and incubated overnight at 4°C. Further enzyme-linked immunosorbent assays were performed using standard procedure as described elsewhere (Noto *et al.*, 2010).

Quantitative real-time reverse transcription polymerase chain reaction

Real-time reverse transcription PCR was performed with a LightCycler 480 (Roche Diagnostics) sequence detection system using LightCycler SYBR Green I at the Quebec genomics Centre. Total RNA was extracted from frozen spinal cord or brain tissues using TRIzol® reagent (Invitrogen). Total RNA was treated with DNase (Qiagen) to get rid of genomic DNA contaminations. Total RNA was then quantified using a NanoDrop spectrophotometer and its purity verified by Bioanalyzer 2100 (Agilent Technologies). Gene-specific primers were constructed using the GeneTools (Biotools Inc.) software v.3. Genes *Atp5* and *GAPDH* were used as internal controls. The primers used for the analysis of genes are given in Table 2. The presence of glial fibrillary acidic protein (GFAP)-luciferase (luc) transgene was assessed by PCR with HotStar Taq Mastermix Kit (Quiagen, Mississauga, ON, Canada) in 15 mM $MgCl_2$ PCR buffer with the following primers: 5′GAAATGTCCGTTCGGTTGGCAGAAGC and 5′CCAAAACCGTGATGGAATGGAACAACA (Keller *et al.*, 2009, 2010).

Barnes maze task

For spatial learning test, the Barnes maze task was performed as described previously (Prut *et al.*, 2007). The animals were subjected to four trials per session with an intertrial interval of 15 min. The probe trial takes 90 s (half of the time used for the training trials) per mouse. Twelve days after the first probe, trial mice are tested again in a second probe trial that takes 90 s per mouse. Mice are not tested between the two probe trials. The time taken by the individual mice to reach the platform was recorded as the primary latency period using video tracking software (ANY-maze).

Step-through passive avoidance test

A two-compartment step-through passive avoidance apparatus (Ugo Basile) was used. The apparatus is divided into bright and dark compartments by a wall with a guillotine door. The bright compartment was illuminated by a fluorescent light (8 W). Mice at various ages were

Table 2 Primers for quantitative real-time PCR

Gene symbol	Forward primer sequences	Reverse primer sequences
Tumour necrosis factor-α	CCAGACCCTCACACTCAGATCATC	CCTTGAAGAGAACCTGGGAGTAGAC
Interleukin-6	GTCCTTCCTACCCCAATTTCCAA	GAATGTCCACAAACTGATATGCTTAGG
Interleukin-1β	GCCCATCCTCTGTGACTCAT	CGACAAAATACCTGTGGCCT
Nox2	TTGGAATTGCAGATGAGGAAGCGAG	CGATCCTGGGCATTGGTGAGT
Interleukin-4	AGATCATCGGCATTTTGAACGAGG	CACTCTCTGTGGTGTTCTTCGTTG
Interleukin-2	CAGCAGCAGCAGCAGCAGCAGC	CCTGGGGAGTTTCAGGTTCCTGTAAT
MCP-1	CCAGATGCAGTTAACGCCCCACTCACCT	TGCTGGTGATCCTCTTGTAGCTCTCCA
Per61	AGAGGAGTGGTATAAGTCGAAATATGC	CCCATCCACCTCGCACATCAG
Per58	TGGCCCTGGACATCGAGATAG	GCTCCATCTCAGGCACAGTCG
Per56	GGATCTCAGTGCCGGTTCATT	GGACTCTGTCACCACCTCCC
Human TDP-43	TTGACCCTTTTGAGATGGAACTTT	ATTTGACTTGAGACAACTTTTCAAATAAGT
Mouse TDP-43	ATTTGAGTCTCCAGGTGGGTGTGG	GTTTCACTATACCCAGCCCACTTTTCTTAGG
Atp5	GCTATGCAACCGCCCTGTACTCTG	ACGGTGCGCTTGATGTAGGGATTC
GAPDH	GGCTGCCCAGAACATCATCCCT	ATGCCTGCTTCACCACCTTCTTG

placed in the bright compartment and allowed to explore for 30 s, at which point the guillotine door was raised to allow the mice to enter the dark compartment. When the mice entered the dark compartment, the guillotine door was closed and an electrical foot shock (0.6 mA) was delivered for 4 s on the second day. On the test (third) day, mice were placed in the bright compartment, no shock was given, and their delay in latency to enter the dark compartment was recorded. The procedure was repeated every month to test the mice at different ages.

Neuromuscular junction staining and count

For monitoring the neuromuscular junctions, 25 mm thick muscle sections were incubated for 1 h in 0.1 M glycine in phosphate buffered saline for 2 h at room temperature and then stained with Alexa Fluor 594-conjugated α-bungarotoxin (1:2000, Molecular Probes/Invitrogen Detection Technologies) diluted in 3% bovine serum albumin in phosphate buffered saline for 3 h at room temperature. After washing in phosphate buffered saline, the muscle sections were blocked in 3% bovine serum albumin, 10% goat serum and 0.5% Triton X-100 in phosphate buffered saline overnight at 48°C. The next day, the sections were incubated with mouse anti-neurofilament antibody 160 K (1:2000, Temecula) and mouse anti-synaptophysin (Dako) in the same blocking solution overnight at 48°C. After washing for 5 h, muscle sections were incubated with goat anti-mouse Alexa Fluor 488-conjugated secondary antibody (Probes/Invitrogen Detection Technologies) diluted 1:500 in blocking buffer for 3 h at room temperature. Three hundred neuromuscular junctions were counted per animal sample, discriminating both innervated and denervated junctions as described above. Frequencies of innervation, partial denervation and denervation were then converted to percentages for statistical analyses ($n = 5$, two-way ANOVA with Bonferroni post-test).

Accelerating rotarod

Accelerating rotarod was performed on mice at 4 rpm speed with 0.25 rpm/s acceleration as described elsewhere (Gros-Louis *et al.*, 2008). Mice were subjected to three trials per session and every 2 weeks.

In vivo bioluminescence imaging

As previously described (Keller *et al.*, 2009, 2010), the images were gathered using IVIS® 200 Imaging System (CaliperLS, Xenogen). Twenty-five minutes prior to the imaging session, the mice received intraperitoneal injection of the luciferase substrate D-luciferine [150 mg/kg for mice between 20 and 25 g; 150–187.5 ml of a solution of 20 mg/ml of D-luciferine dissolved in 0.9% saline was injected (CaliperLS, Xenogen)].

Statistical analysis

For statistical analysis, the data obtained from independent experiments are presented as the mean ± SEM. A two-way ANOVA with repeated measures was used to study the effect of group (transgenic and non-transgenic mice) and time (in months or weeks) on latency to fall (accelerating rotarod test), latency to go to the dark chamber (passive avoidance test), primary errors and primary latency (Barnes maze test). Two-way ANOVA with repeated measures was also used for axonal calibre distribution and total flux of photons for *in vivo* imaging. The mixed procedure of the SAS software version 9.2 (SAS Institute Inc.) was used with a repeated statement and covariance structure that minimize the Akaike information criterion. The method of Kenward–Roger was used to calculate degrees of freedom. Pairwise comparisons were made using Bonferroni adjustment. A one-way ANOVA was performed using GraphPad Prism software version 5.0 for real-time inflammation array, real-time reverse transcription PCR and neurofilament enzyme-linked immunosorbent analysis. *Post hoc* comparisons were performed by Tukey's test, with a statistical significance of $P < 0.05$.

Results

Generation of transgenic mice carrying genomic TDP-43 fragments

We generated three transgenic mouse models using genomic DNA fragments coding for either wild-type TDP-43, TDP-43^{A315T} or TDP-43^{G348C} carrying mutations linked to human familial

amyotrophic lateral sclerosis (Kabashi *et al.*, 2008). The transgenic mice (wild-type, A315T and G348C) were generated by injection of DNA fragments into one-cell embryos, subcloned from *TARDBP* bacterial artificial chromosomes using the endogenous ~4 kB promoter. The A315T and G348C mutations were inserted using site-directed mutagenesis (Fig. 1A). Founder TDP-43 transgenic mice were identified by the presence of the 1.8-kb EcoRV fragment on the Southern blot (Supplementary Fig. 1A). Real-time PCR analysis of the spinal cord lysates of wild-type TDP-43, TDP-43^{A315T} and TDP-43^{G348C} mice revealed bands corresponding to human TDP-43 (Supplementary Fig. 1B). As shown by immunoblot analysis, the human TDP-43 transgenes (wild-type and mutants) were expressed in all the tissues examined (Fig. 1B). Real-time reverse transcription PCR showed that the messenger RNA expression of human TDP-43 in the spinal cord was elevated by ~3-fold in 3-month-old wild-type TDP-43, TDP-43^{A315T} and TDP-43^{G348C} transgenic mice as compared with the endogenous mouse TDP-43 (Fig. 1C). Whereas expression of human TDP-43 messenger RNA transcripts remained constant with age, the levels of endogenous mouse TDP-43 messenger RNA transcripts were decreased significantly in 10-month-old transgenic mice (wild-type TDP-43, TDP-43^{A315T} and TDP-43^{G348C}) as compared with 3-month-old mice ($^{*}P < 0.01$, Supplementary Fig. 1E). This is consistent with TDP-43 autoregulation through TDP-43 binding and splicing-dependent RNA degradation as described previously (Polymenidou *et al.*, 2011). Next, we examined whether we can detect pathological cytosolic TDP-43 in our transgenic models, characteristic of amyotrophic lateral sclerosis.

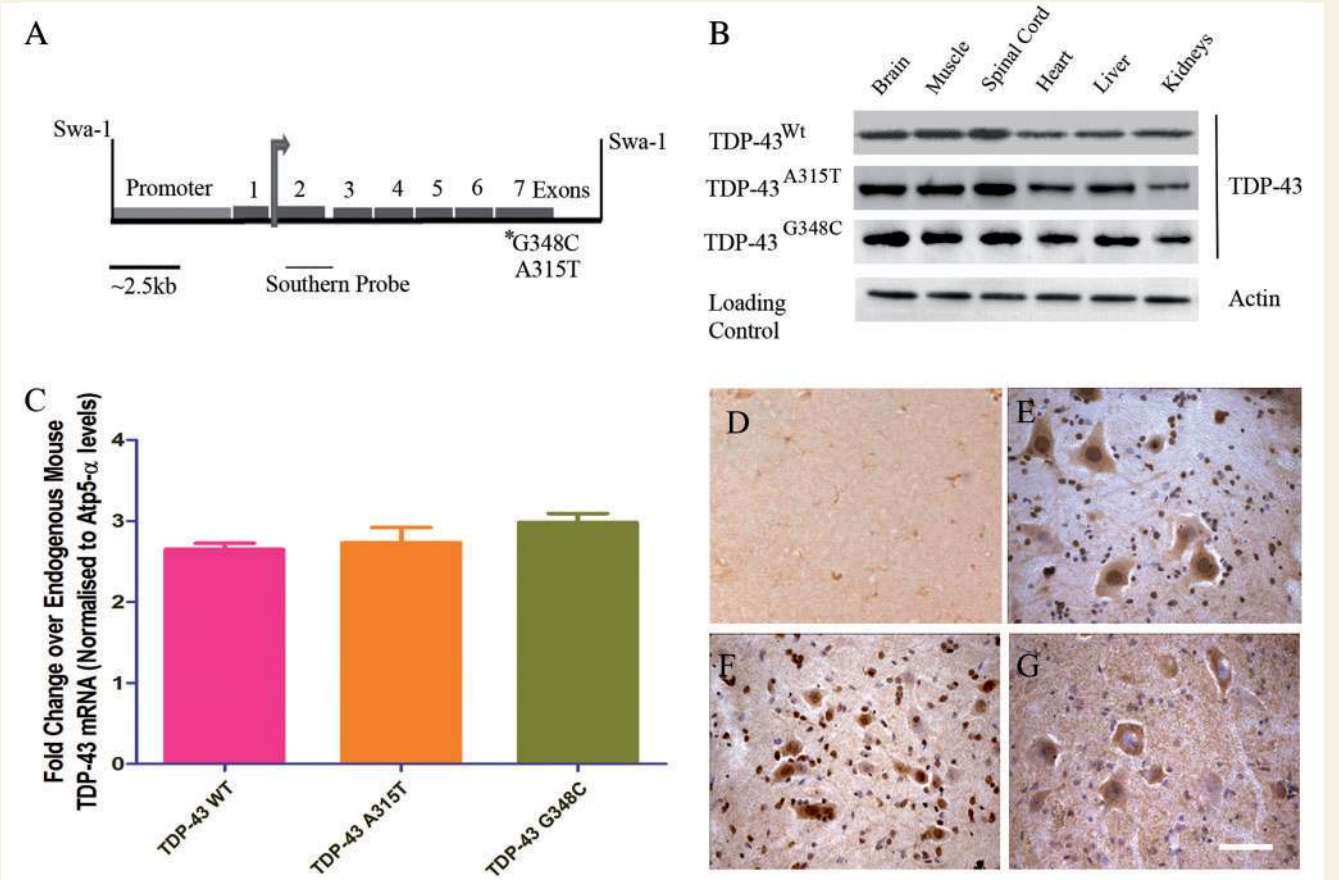

Figure 1 Generation and characterization of TDP-43 transgenic mice. (**A**) Map of human *TARDBP* gene (Gene ID: 23435) showing upstream ~4 kb promoter (uncharacterized) and various exons (numbered 1–7) and introns. The orientation of transcription is shown by arrow. Asterisk denotes position of two mutations G348C (1176G > T) and A315T (1077G > A). The approximate locations of the Southern blotting probes are also indicated. (**B**) Western blots from lysates of various tissues from wild-type TDP-43, TDP-43^{A315T} and TDP-43^{G348C} transgenic mice at 2 months of age using mouse monoclonal TDP-43 antibody that detect human TDP-43 only. Actin is shown as loading control. (**C**) Quantitative real-time PCR analysis of human TDP-43 messenger RNA expression in the spinal cord of wild-type TDP-43, TDP-43^{A315T} and TDP-43^{G348C} transgenic mice at 2 months of age compared individually to their wild-type littermates and normalized to Atp-5α levels. Data shown are means ± SEM of five different mice from each group. (**D–G**) Immunohistochemistry shows human TDP-43 expression pattern in the spinal cord of ~8-month-old wild-type TDP-43, TDP-43^{A315T} and TDP-43^{G348C} transgenic mice using TDP-43 monoclonal antibody. It is noteworthy that the expression of TDP-43 is mostly nuclear in wild-type TDP-43 mice (**E**), but TDP-43 is localized in the cytoplasm in TDP-43^{G348C} mice (**G**), and to a lesser extent in TDP-43^{A315T} mice (**F**). TDP-43 monoclonal antibody does not recognize endogenous mouse TDP-43 in non-transgenic control mice (**D**). Scale bar = 20 μm.

The immunohistochemical staining with anti-human TDP-43 antibodies of spinal cord sections from 10-month-old transgenic mice revealed a cytoplasmic accumulation of TDP-43 in TDP-43^{G348C} mice and to a lower extent in TDP-43^{A315T} mice (Fig. 1D–G and Supplementary Fig. 3A and B). In contrast, the TDP-43 localization remained mostly nuclear in wild-type TDP-43 and non-transgenic mice.

Overexpression of wild-type and mutant TDP-43 is associated with the formation of cytosolic aggregates

Biochemically, amyotrophic lateral sclerosis and FTLD-U cases are characterized by 25 kDa C-terminal deposits that might contribute to pathogenesis (Cairns *et al.*, 2007). Similar to amyotrophic lateral sclerosis cases, TDP-43^{G348C} and TDP-43^{A315T} mice had ~25 kDa fragments in the spinal cord (Fig. 2A and B). This ~25 kDa fragment was more prominent at 10 months of age (Fig. 2B) than at 3 months of age (Fig. 2A). Blots probed with human TDP-43-specific monoclonal antibody reveal increased cytotoxic ~25 kDa TDP-43 fragments in the brain (Supplementary Fig. 1E and F) and spinal cord (Supplementary Fig. 1C and D) lysates of TDP-43^{G348C} and TDP-43^{A315T} mice at 10 months of age as compared with 3-month-old mice. Using immunofluorescence and monoclonal TDP-43 antibody, we detected the presence of cytoplasmic TDP-43 aggregates in TDP-43^{G348C} mice (Fig. 2H) and TDP-43^{A315T} (Fig. 2G) mice at around 10 months of age, but not in wild-type TDP-43 mice (Fig. 2F). Cytoplasmic localization as well as aggregates of TDP-43 were age dependent as they were absent in the spinal cord sections of 3-month-old mice (Fig. 2C–E). In order to determine if the TDP-43 aggregates were ubiquitinated, we performed double immunofluorescence with TDP-43 and anti-ubiquitin antibodies. We found that ubiquitin specifically co-localized with cytoplasmic TDP-43 aggregates in the spinal cord (Fig. 2L–N), hippocampal (Fig. 2O–Q) and cortical sections (Fig. 2R–T) of 10-month-old TDP-43^{G348C} mice, but not in the spinal cord sections of 3-month-old (Fig. 2I–K) TDP-43^{G348C} mice. Ubiquitination of TDP-43-positive inclusions was further confirmed by the co-immunoprecipitation of ubiquitin (poly-ubiquitin) with human TDP-43. This immunoprecipitation experiment clearly demonstrates that proteins associated with TDP-43 inclusions especially in 10-month-old TDP-43^{G348C} and TDP-43^{A315T} mice are massively ubiquitinated (Fig. 2U). However, probing the blot with anti-human TDP-43 monoclonal antibody (Fig. 2U) or with polyclonal antiTDP-43 (data not shown) did not reveal high molecular weight forms of TDP-43, suggesting that TDP-43 itself was not ubiquitinated. To further address this question, we carried out immunoprecipitation of spinal cord extracts with anti-ubiquitin and probed the blot with anti-TDP-43 monoclonal antibody (Fig. 2U). As expected, TDP-43 was co-immunoprecipitated with anti-ubiquitin. However, only a small amount of high molecular weight forms of TDP-43 (i.e. poly-ubiquitinated) could be detected (Fig. 2V). This result is consistent with a report that TDP-43 is not, in fact, the major ubiquitinated target in ubiquitinated inclusions of amyotrophic lateral sclerosis (Sanelli *et al.*, 2007).

Peripherin overexpression and neurofilament disorganization in TDP-43 transgenic mice

A pathological hallmark of both sporadic and familial amyotrophic lateral sclerosis is the presence of abnormal accumulations of neurofilament and peripherin proteins in motor neurons (Carpenter, 1968; Corbo and Hays, 1992; Migheli *et al.*, 1993). Here, we investigated whether such cytoskeletal abnormalities appear in the large motor neurons of TDP-43 transgenic mice. Immunofluorescence analysis of the spinal cord sections by anti-peripherin polyclonal antibody revealed the presence of peripherin aggregates in large motor neurons of TDP-43^{G348C}, TDP-43^{A315T} and, to a lesser extent, in wild-type TDP-43 mice at 10 months of age as compared with 3-month-old mice (Fig. 3A–E and Supplementary Fig. 2A–D). Further analysis revealed that peripherin aggregates were also present in the brain. The aggregates in TDP-43^{G348C} and, to a lesser extent, in TDP-43^{A315T} and wild-type TDP-43 mice were localized in the hippocampus (Fig. 3F–J) and cortex (Fig. 3K–O). Western blot analysis of the brain lysates of transgenic mice using polyclonal antibody against peripherin revealed abnormal splicing variants of peripherin in TDP-43^{G348C} and TDP-43^{A315T} transgenic mice, including a toxic Per61 fragment (Fig. 3P) along with other fragments like Per56 and the normal Per58. The use of anti-peripherin monoclonal antibody revealed overexpression of the peripherin ~58 kDa fragment in TDP-43^{G348C}, TDP-43^{A315T} and to a lower extent in wild-type TDP-43 mice compared with non-transgenic mice.

Earlier reports have shown that Per61 is neurotoxic and is present in spinal cords of patients with amyotrophic lateral sclerosis (Robertson *et al.*, 2003). We then determined the messenger RNA expression levels in the spinal cord extracts of various peripherin transcripts (Per61, Per58 and Per56) using real-time PCR. Though the levels of Per58 and Per56 are not significantly different between various transgenic mice, the levels of Per61 are significantly upregulated (~2.5-fold, $P < 0.01$) in TDP-43^{G348C} mice compared with wild-type TDP-43 mice (Fig. 3Q). Per61 was also upregulated in TDP-43^{A315T} mice (~1.5-fold) compared with wild-type TDP-43 mice. Antibody specifically recognizing Per61 was used to detect Per61 in the spinal cord sections of TDP-43^{G348C} mice (Fig. 3S) and in wild-type TDP-43 mice (Fig. 3R). As expected, Per61 antibody stained Per61 aggregates in the axons and cell bodies in human amyotrophic lateral sclerosis spinal cord sections (Fig. 3U) but not control spinal cord tissues (Fig. 3T).

The TDP-43 transgenic mice also exhibit altered levels of peripherin and neurofilament protein expression. As shown in Fig. 4A, western blotting revealed that heavy neurofilament protein is downregulated by ~1.5-fold and light neurofilament protein by ~2-fold in the spinal cord extracts of 10-month-old TDP-43^{G348C} mice as compared with non-transgenic mice (Fig. 4A). The levels of medium neurofilament protein on the other hand were not significantly altered in any of the transgenic mice. We determined neurofilament levels in the spinal cords of 10-month-old transgenic and non-transgenic mice using enzyme-linked immunosorbent assay. Usual enzyme-linked immunosorbent assay methods are not suitable for the quantitative measurement of

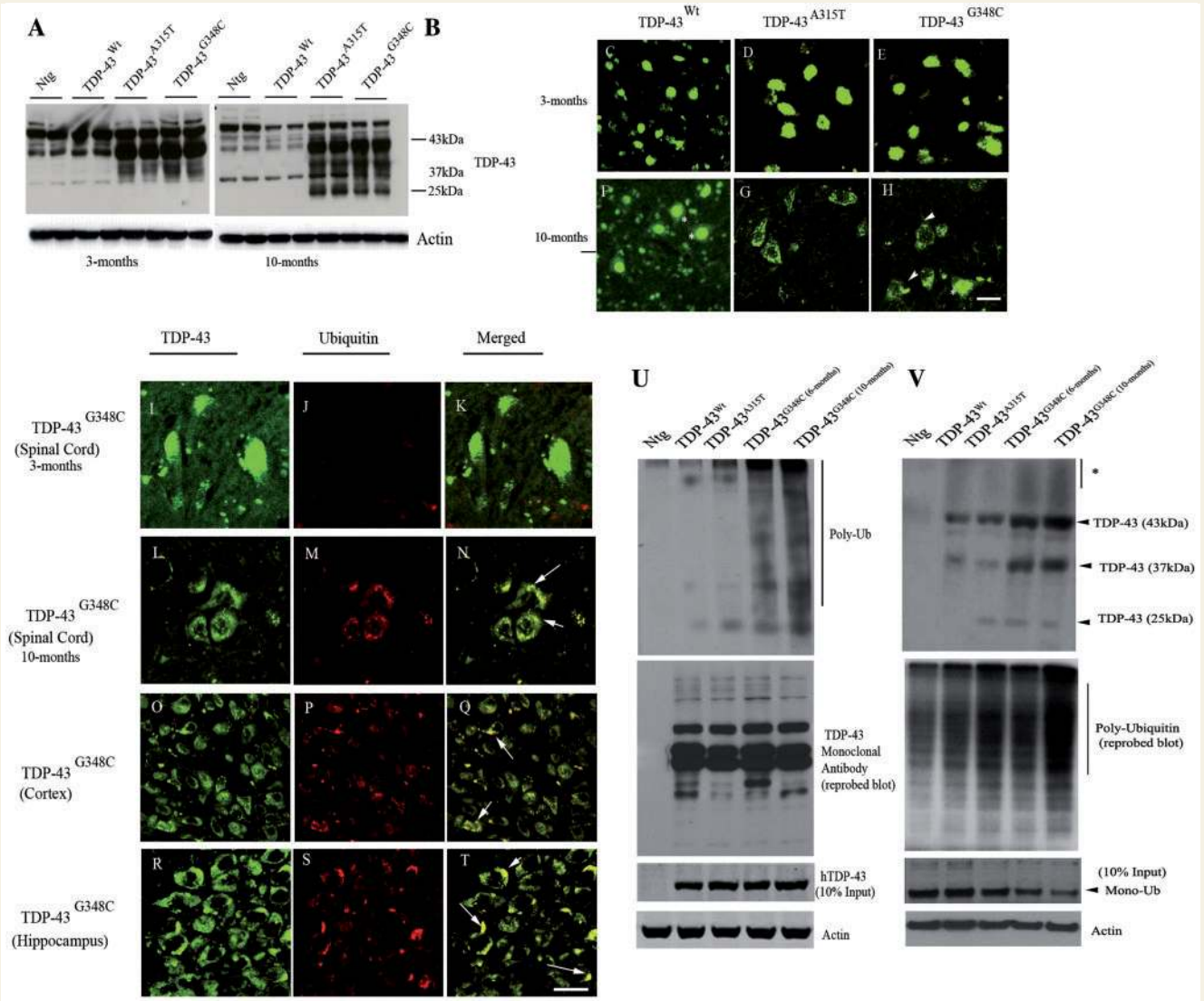

Figure 2 Biochemical and pathological features of amyotrophic lateral sclerosis/FTLD in TDP-43 transgenic mice. (**A** and **B**) Western blot of spinal cord lysates from Ntg (non-transgenic), wild-type (Wt) TDP-43, TDP-43^{A315T} and TDP-43^{G348C} mice using polyclonal TDP-43 antibody at 3 and 10 months show that TDP-43 (both G348C and A315T mutants) have ~35 and ~25 kDa fragments that increase with age. Actin is shown as a loading control. (**C–H**) Immunofluorescence of the spinal cord of 10-month-old wild-type TDP-43 (**F**), TDP-43^{A315T} (**G**) and TDP-43^{G348C} mice (**H**) using TDP-43 monoclonal antibody show cytoplasmic human TDP-43 aggregates (arrowheads) especially in the spinal cord sections of TDP-43^{G348C} transgenic mice. Some of the TDP-43 is still in nucleus (asterisk). On the other hand, spinal cord sections of 3-month-old transgenic mice show nuclear staining exclusively (**C–E**). (**I–T**) Double immunofluorescence of the brain and spinal cord sections of 10-month-old TDP-43^{G348C} mice using monoclonal TDP-43 antibody and anti-ubiquitin antibody show ubiquitinated TDP-43 aggregates (arrows) in spinal cord (**L–N**), cortex (**O–Q**) and hippocampal (**R–T**) regions. (**I–K**) Spinal cord sections of 3-month-old TDP-43^{G348C} mice do not show intense ubiquitination. Background intensities were matched with 10-month-old mice for consistency. (**U**) Co-immunoprecipitation of ubiquitin using mouse monoclonal TDP-43 from spinal cord lysates of transgenic mice show that proteins associated with human TDP-43 are poly-ubiquitinated (Poly-Ub) more in TDP-43^{G348C} mice. Note that the ubiquitination is higher in 10-month-old mice than in 6-month old TDP-43^{G348C} mice. Re-probed western blot is shown for TDP-43 using monoclonal antibody. Western blot of human TDP-43 using monoclonal antibody is shown as 10% input and actin as loading control. (**V**) Reverse co-immunoprecipitation with anti-ubiquitin antibody shows that TDP-43 was co-immunoprecipitated with anti-ubiquitin. However, only a small amount of high molecular weight forms of TDP-43 (i.e. poly-ubiquitinated) could be detected. Western blot of ubiquitin using polyclonal antibody is shown as 10% input and actin as loading control. Scale bar = 50 μm (**C–H**); 25 μm (**I–T**).

neurofilament proteins because of their insolubility. However, neurofilament proteins are dissolved in urea at high concentration. Standard curves of light, medium and heavy neurofilament proteins dissolved in various concentrations of urea diluted with the dilution buffer were prepared as described elsewhere (Lu *et al.*, 2011) (Supplementary Fig. 4A–C). A suitable concentration of urea for detection was estimated to be ~0.3 mol/l, because the sensitivity was higher in 0.3 mol/l urea than in the other concentrations

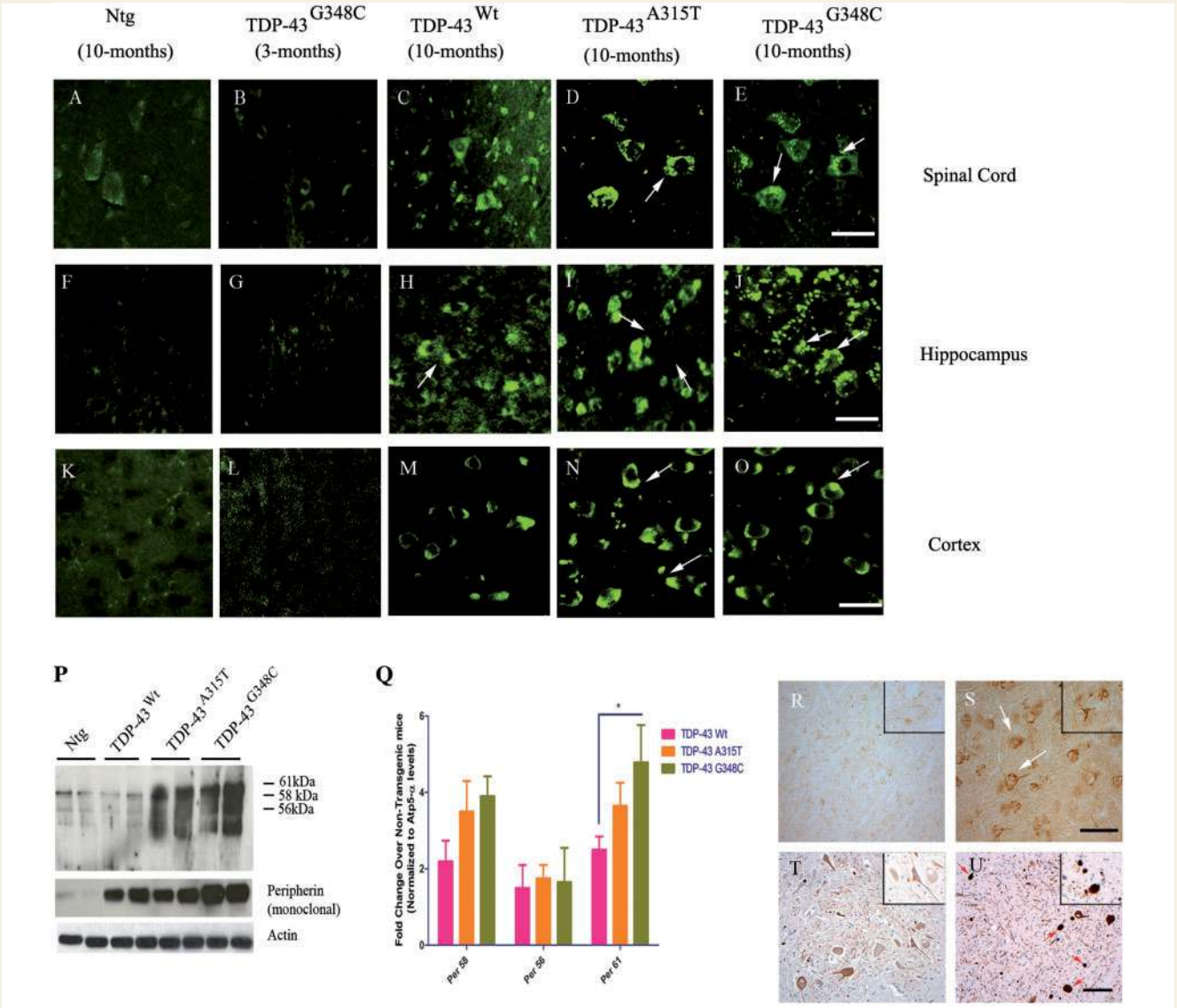

Figure 3 Peripherin abnormalities in TDP-43 transgenic mice. (**A–O**) Immunofluorescence of the brain (**F–O**) and spinal cord (**A–E**) sections of 10-month-old non-transgenic (Ntg), wild-type (Wt) TDP-43, TDP-43^{A315T} and TDP-43^{G348C} transgenic mice using polyclonal anti-peripherin antibody. Peripherin immunofluorescence of the spinal cord sections show peripherin aggregates more in TDP-43^{G348C} mice (**E**) (arrow), and also some in TDP-43^{A315T} mice (**C**) and much less in wild-type TDP-43 mice (**C**) as compared with non-transgenic control (**A**). Spinal cord sections of 3-month-old TDP-43^{G348C} mice do not show peripherin overexpression or aggregates (**B**). (**F–J**) Hippocampal region of the brain of 10-month-oldTDP-43^{G348C} mice show abundant peripherin aggregates (**J**). Peripherin aggregates are also seen to a lesser extent in TDP-43^{A315T} mice (**I**) and much less in wild-type TDP-43 mice (**H**) as compared with non-transgenic control (**F**) and 3-month-old TDP-43G348C mice (**G**). (**K–O**) Similarly, peripherin immunofluorescence in 10-month-old TDP-43^{G348C} mice (**O**) in the cortical region of the brain show peripherin aggregates. These aggregates are also seen to a lesser extent in TDP-43^{A315T} mice (**N**) and much less in wild-type TDP-43 mice (**M**) as compared with non-transgenic control (**K**) and 3-month-old TDP-43G348C mice (**L**). (**P**) Western blot analysis of the brain lysates of 10-month-old non-transgenic, wild-type TDP-43, TDP-43^{A315T} and TDP-43^{G348C} transgenic mice using polyclonal peripherin antibody reveal various peripherin splice variants including the Per61, Per58 and Per56 fragments especially in TDP-43^{G348C} mice. Monoclonal peripherin antibody revealed overexpression of peripherin in TDP-43^{G348C}, TDP-43^{A315T} and to a lesser extent in wild-type TDP-43 mice as compared with non-transgenic control. Actin is shown as loading control. (**Q**) Quantitative real-time PCR analysis of messenger RNA levels of peripherin splice variants Per61, Per58 and Per56 in the spinal cord lysates show that TDP-43^{G348C} mice had ~2.5-fold higher Per61 transcript levels than in wild-type TDP-43 spinal cord. Per58 levels are also higher in TDP-43^{G348C} mice compared with wild-type TDP-43 mice, but no significant differences are observed in Per56 levels between different transgenic mice. Peripherin transcript levels are expressed as fold change over non-transgenic controls normalized to Atp-5α levels. One-way ANOVA was used with Tukey's *post hoc* comparison for statistical analysis ($n = 3$), $^*P < 0.01$ (**R–U**) Immunohistochemistry on spinal cord tissues using Per61-specific antibody reveal Per61-specific aggregates in TDP-43^{G348C} mice (**S**) similar to sporadic amyotrophic lateral sclerosis spinal cord tissues (**U**). In contrast, Per61 antibody yielded weak staining of the spinal cord in human control (**T**) and in wild-type TDP-43 transgenic mice (**R**). Inset showing higher magnification images. Scale bars = 25 μm (**A–O**); 50 μm (**R–U**).

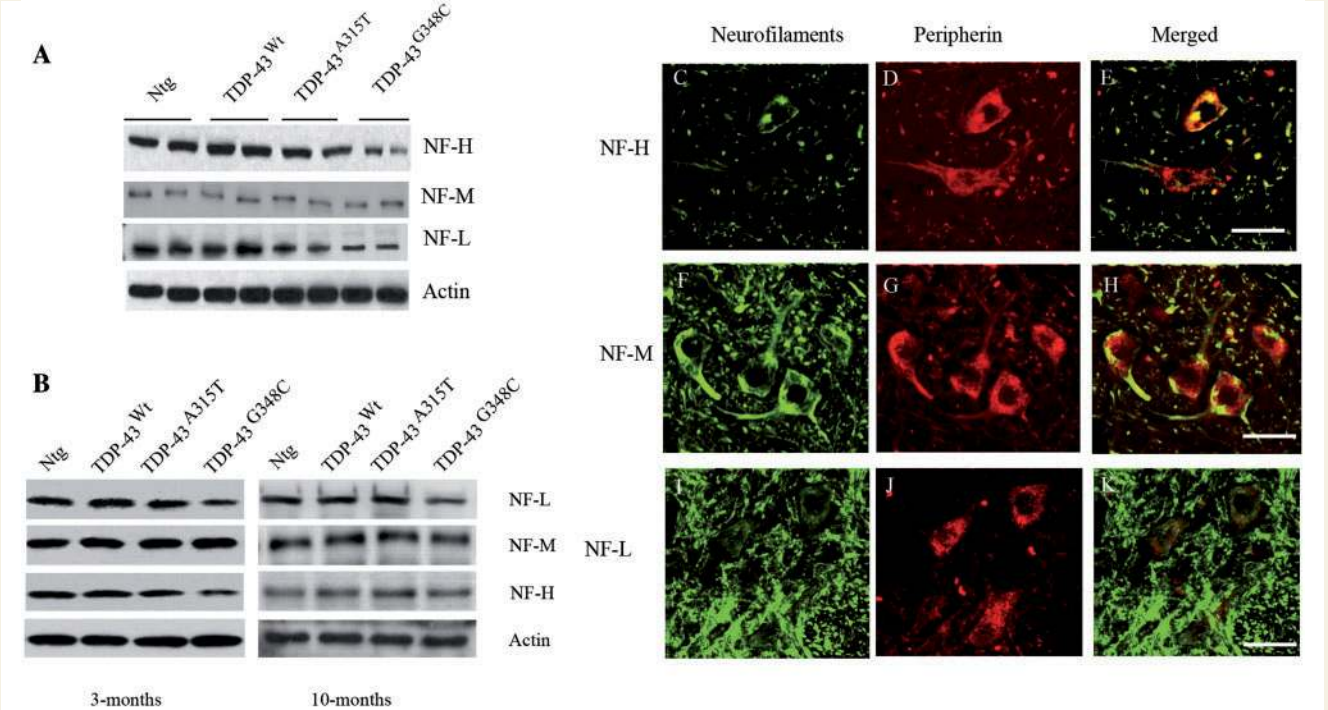

Figure 4 Neurofilament abnormalities in TDP-43 transgenic mice. (**A**) Western blots of various neurofilament proteins on the spinal cord lysates of 10-month-old non-transgenic (Ntg), wild-type (Wt) TDP-43, TDP-43^{A315T} and TDP-43^{G348C} transgenic mice using heavy neurofilament protein (NF-H), medium neurofilament protein (NF-M) and light neurofilament protein (NF-L) specific antibodies. Note the sharp reduction in the protein levels of light neurofilament protein and heavy neurofilament protein in TDP-43^{G348C} spinal cord lysates as compared with wild-type TDP-43 lysates. Actin is shown as loading control. (**B**) Western blots of various neurofilament proteins on the spinal cord lysates of 3-month and 10-month-old non-transgenic, wild-type TDP-43, TDP-43^{A315T} and TDP-43^{G348C} transgenic mice using heavy neurofilament protein, medium neurofilament protein and light neurofilament protein-specific antibodies. Actin is shown as loading control. (**C–K**) Double immunofluorescence of various neurofilaments (green)—heavy neurofilament protein (**C**), medium neurofilament protein (**F**) and light neurofilament protein (**I**) with polyclonal peripherin antibody (red) on the TDP-43^{G348C} spinal cord sections reveal that heavy neurofilament protein is recruited to peripherin aggregates (arrows, **E**), and to a lesser extent heavy neurofilament protein (**H**), but not light neurofilament protein (**K**). Scale bar = 25 μm.

examined. Analysis of enzyme-linked immunosorbent assay revealed that light neurofilament protein levels are significantly reduced in 10-month-old TDP-43G348C mice as compared with age-matched non-transgenic controls ($^{**}P < 0.001$, Supplementary Fig. 4D). Ten-month-old spinal cord samples were fractionated in detergent soluble and insoluble fractions. Though most of the neurofilament proteins were in detergent insoluble fraction, peripherin levels could be detected in both soluble and insoluble fractions (Supplementary Fig. 5A and B). We also determined the heavy neurofilament protein, medium neurofilament protein and light neurofilament protein levels in the sciatic nerve of 3 and 10-month-old transgenic mice. We observed a slight decrease in light neurofilament protein levels in 3-month-old TDP-43^{G348C} mice as compared with age-matched wild-type TDP-43 and TDP-43^{A315T} mice, which had levels similar to non-transgenic mice (Fig. 4B). At 10 months of age, TDP-43^{G348C} mice had ~50% reduction in light neurofilament protein levels in the sciatic nerve (Fig. 4B) as compared with wild-type TDP-43 mice. We then used double immunofluorescence techniques to determine which neurofilament forms part of the aggregates with peripherin in TDP-43^{G348C} spinal cord sections. We found that heavy neurofilament protein clearly forms part of the aggregates (Fig. 4C–E), followed by medium neurofilament protein to a lesser extent (Fig. 4F–H) and light neurofilament protein (Fig. 4I–K) does not form part of the aggregates. TDP-43 aggregates co-localize partially with heavy neurofilament protein and medium neurofilament protein, but not with light neurofilament protein (Supplementary Fig. 6A–C).

Smaller calibre of peripheral axons in TDP-43 transgenic mice

Our previous work has demonstrated that overexpression of the wild-type peripherin, especially in context of light neurofilament protein loss, leads to a late onset motor neuron disease and axonal degeneration (Beaulieu *et al.*, 1999). To investigate whether similar pathology was associated with peripherin induction in TDP-43 transgenic mice, we analysed at different time points the number of axons, the distribution of axonal calibre and their morphology. Axonal counts of the L5 ventral root from TDP-43 transgenic mice at 10 months of age failed to reveal any significant differences in the number of motor axons (Fig. 5A–E). Normal mice exhibit a

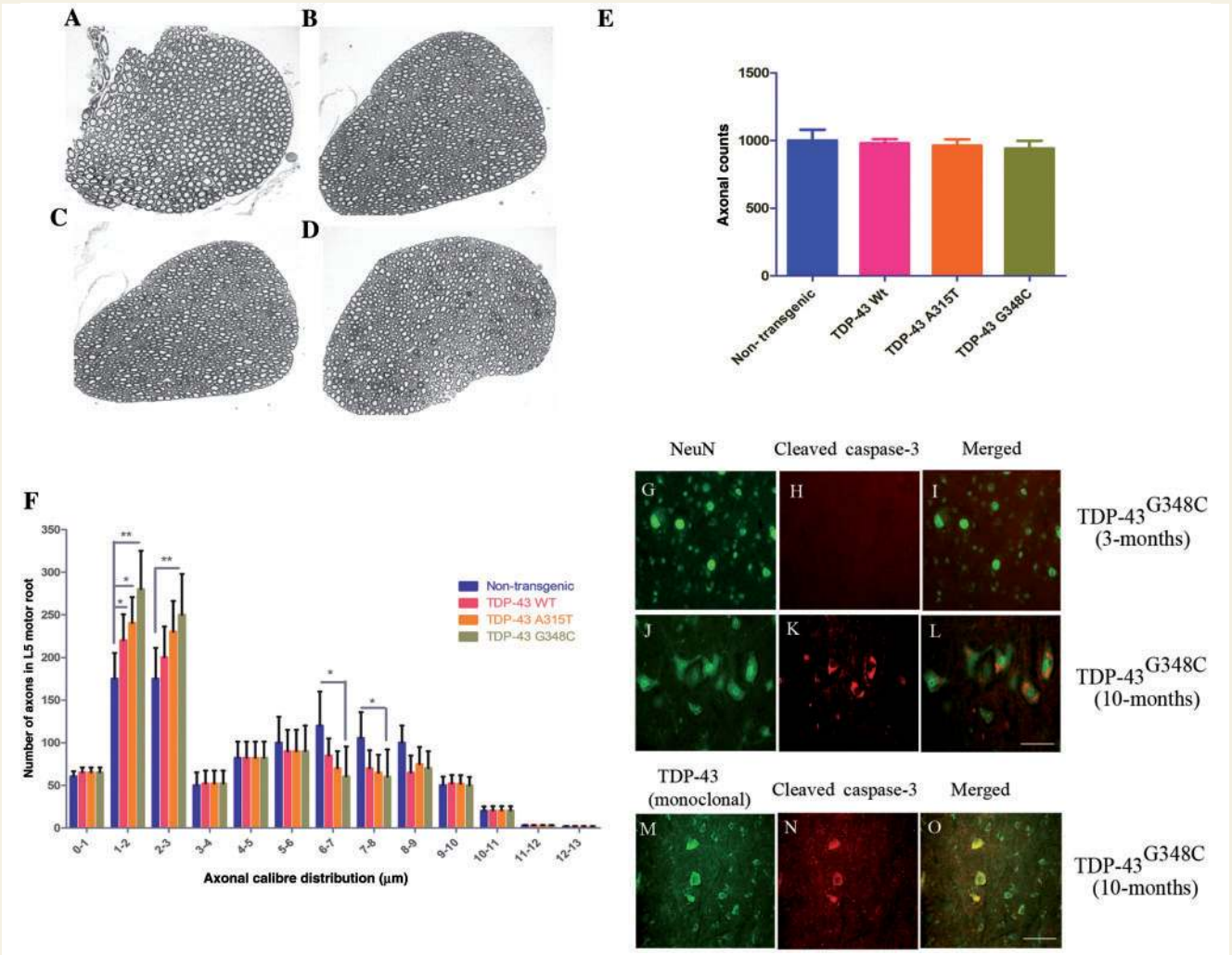

Figure 5 Reduced axonal calibre in ventral roots of TDP-43 transgenic mice. (**A–D**) Toluidine blue staining of thin sections of L5 ventral root axons from non-transgenic (**A**), wild-type TDP-43 (**B**), TDP-43^{A315T} (**C**) and TDP-43^{G348C} (**D**) mice showing no significant differences in the motor neuron count. (**E**) Axonal counts of transgenic mouse at 10 months of age failed to reveal any significant differences in the number of motor axons in the L5 ventral root. (**F**) Cumulative axon calibre distribution of axons at L5 ventral root of 10-month-old non-transgenic and transgenic mice showing increased number of 1–3 μm axons and reduced number of 6–9 μm axons in TDP-43^{G348C} mice. A two-way ANOVA with repeated measures was used to study the effect of group (transgenic and non-transgenic mice) on axonal calibre distribution. Pairwise comparisons were made using Bonferroni adjustment $*P < 0.01$ and $**P < 0.001$. Data shown are means ± SEM of five different mice from each group. (**G–L**) Double immunofluorescence using neuronal nuclei (NeuN; a neuronal marker) and cleaved caspase-3 show many cleaved caspase-3 positive neurons in the spinal cord of TDP-43^{G348C} mice at 10 months of age (**L**) compared with 3-month-old TDP-43^{G348C} mice (**I**). (**M–O**) Double immunofluorescence using human-specific TDP-43 and cleaved caspase-3 show many cleaved caspase-3 positive neurons in the spinal cord of TDP-43^{G348C} mice at 10 months of age. Scale bar = 25 μm.

bimodal distribution of axonal calibre with peaks at ~2 and ~7 μm in diameter (Fig. 5F). In contrast, a skewed bimodal distribution is observed in TDP-43 transgenic mice. There was a 10% increase (an increase of 100 axons, $P < 0.001$) in the number of motor axons with 1–3 μm calibre and a 12% decrease (a decrease of 120 axons) in the number of motor axons with 6–9 μm calibre in 10-month-old TDP-43^{G348C} mice compared with non-transgenic mice (Fig. 5F). There was a similar 7% increase (an increase of 70 axons, $P < 0.01$) in the number of motor axons with 1–3 μm calibre and an 8% decrease (a decrease of 80 axons) in the number of motor axons with 6–9 μm calibre in 10-month-old TDP-43^{A315T} mice as compared with non-transgenic mice. The increase in the number of motor axons with 1–3 μm calibre was less (~5%) and a slight decrease of 6% in 10-month-old wild-type TDP-43 mice compared with non-transgenic mice (Fig. 5F). We have quantified the functional neuromuscular junctions through fluorescence staining for pre- and postsynaptic markers. Neuromuscular junction count revealed that 5 ± 4% of the analysed neuromuscular junctions were denervated in 10-month-old wild-type TDP-43 mice and 10 ± 5% were denervated in age-matched TDP-43^{G348C} mice as compared with non-transgenic controls (Supplementary Fig. 7D). Furthermore, over 20% of

neuromuscular junctions were partially denervated in both wild-type TDP-43 mice and TDP-43^{G348C} mice.

The severe alterations in motor axon morphology of TDP-43^{G348C} mice prompted us to examine whether this phenomenon was associated with caspase-3 activation, a sign of neuronal damage. Using double immunofluorescence and antibodies against cleaved caspase-3 and neuronal nuclei (NeuN; a neuronal marker), we found many cleaved caspase-3 positive neurons in the spinal cord of TDP-43^{G348C} mice at 10 months of age (Fig. 5J–L) compared with 3-month-old TDP-43^{G348C} mice (Fig. 5G–I). Cleaved caspase-3 positive cells were also positive for cytoplasmic TDP-43 (Fig. 5M–O). However, no caspase-3 positive neurons were detected in wild-type TDP-43 and TDP-43^{A315T} mice at 10 months of age (data not shown).

TDP-43 transgenic mice develop motor dysfunction and cognitive deficits

Behavioural analysis of the TDP-43 transgenic mice revealed age-related cognitive defects, particularly learning and memory deficits. We used passive avoidance test to detect deficiencies in contextual memory. No defects were detected until 7 months of age. However, after 7 months, wild-type TDP-43, TDP-43^{A315T} and TDP-43^{G348C} mice exhibited severe cognitive impairments, especially in the 11th and 13th months (Fig. 6A). The most robust memory deficit occurred in TDP-43^{G348C} mice. We then conducted Barnes maze test to specifically discern the spatial learning and memory deficits in these mice. The TDP-43^{G348C} and, to a lesser extent, wild-type TDP-43 mice had significant learning impairment in the Barnes maze test at 10 months of age (Fig. 6B and C) as depicted by significant reduction in the time spent in the target quadrant and increased primary errors. In the probe trial (Day 5), TDP-43^{G348C} and wild-type TDP-43 mice showed a significant reduction in the time spent in the target quadrant and increase in the total number of errors as compared with age-matched non-transgenic mice (Fig. 6B and C). Thus, 10-month-old TDP-43^{G348C} mice had severe spatial learning and memory deficits. Transgenic mice overexpressing TDP-43^{G348C}, TDP-43^{A315T} or wild-type TDP-43 also exhibited age-related motor deficits as depicted by significant reductions in latency in the accelerating rotarod tests starting at ~42 weeks of age (Fig. 6D).

Age-related neuroinflammatory changes in TDP-43 mice precede behavioural defects

The microgliosis and astrogliosis were assessed in spinal cord and brain sections of different transgenic mice at presymptomatic stage (3 months) and after appearance of behavioural and sensorimotor deficits (10 months). Antibodies against ionized calcium binding adaptor molecule 1 (Iba-1), a marker for microglial ion channels, revealed the existence of microgliosis in the brain and spinal cord sections of 10-month-old TDP-43 transgenic mice (Fig. 7A–J). The microgliosis in the brain and spinal cord sections of 10-month-old wild-type TDP-43 and TDP-43^{A315T} mice was less pronounced than in 10-month-old TDP-43^{G348C} mice (Fig. 7E–H). Microgliosis was age dependent as both spinal cord and brain sections of 3-month-old wild-type TDP-43, TDP-43^{A315T} (data not shown) and TDP-43^{G348C} mice (Fig. 7B and G) had far less microglial activation than 10-month-old mice of the same genotype. We also used antibodies against glial fibrillary acidic protein to detect astrogliosis in the brain (Fig. 7P–T) and spinal cord (Fig. 7K–O) sections of 10-month-old TDP-43 transgenic mice. Again, astrogliosis in wild-type TDP-43 and TDP-43^{A315T} mice was less severe than in TDP-43^{G348C} mice. Similar to microgliosis, astrogliosis was also age dependent as both spinal cord and brain sections of 3-month-old wild-type TDP-43, TDP-43^{A315T} (data not shown) and TDP-43^{G348C} mice (Fig. 7L and Q) had far less astroglial activation than 10-month-old mice of same genotype. We then quantified messenger RNA levels of various pro-inflammatory cytokines and chemokines in the spinal cord of 10-month-old transgenic mice using quantitative real-time PCR. The messenger RNA levels of all studied cytokines and chemokines were upregulated in wild-type TDP-43, TDP-43^{A315T} and TDP-43^{G348C} mice when compared with their non-transgenic littermates. For instance, the levels of tumour necrosis factor-α (2.7-fold), interleukin-6 (2-fold) and monocyte chemotactic protein-1 (MCP-1; 2.5-fold) were all upregulated in TDP-43^{G348C} mice as compared with wild-type TDP-43 mice (Fig. 7U).

Next, we asked the question whether neuroinflammatory signals can be detected in early, pre-onset stages of the disease. Previous results, using the sensitive live imaging approaches in SOD1 mutant models, revealed that one of the first signs of the disease is the transient induction of the GFAP signals (Keller *et al.*, 2009). To investigate the temporal induction of gliosis and to relate it to sensorimotor and learning deficits, we generated by breeding double transgenic mice carrying a TDP-43 transgene and a GFAP-luc transgene consisting of the luciferase reporter driven by the murine GFAP promoter.

To analyse the spatial and temporal dynamics of astrocytes activation/GFAP induction in TDP-43 mouse model, we performed series of live imaging experiments, starting at early 4–5 weeks of age until 52 weeks. Quantitative analysis of the imaging signals revealed an early (~20 weeks) and significant upregulation of GFAP promoter activity (Fig. 8A–H) in the brain of TDP-43^{G348C}/GFAP-luc mice. Starting at 20 weeks of age, the light signal intensity from the brain of TDP-43^{A315T}/GFAP-luc mice and wild-type TDP-43/GFAP-luc mice was also significantly elevated when compared with wild-type littermates, but the intensity was less than in GFAP-luc/TDP-43^{G348C} mice. The GFAP promoter activity in the brain progressively increased with age until it peaked at ~50 weeks for GFAP-luc/TDP-43^{G348C}, and at ~46 weeks for GFAP-luc/TDP-43^{A315T} (Supplementary Fig. 8) and GFAP-luc/wild-type TDP-43mice (Fig. 8Q). It is noteworthy that the induction of gliosis at 20 weeks in the brain of TDP-43 transgenic mice preceded the cognitive deficits first detected at ~28 weeks (Fig. 6). Likewise, in the spinal cord of all three TDP-43 mouse models, the induction of GFAP promoter activity signals at ~30 weeks of age (Fig. 8I–P and R and Supplementary Fig. 8) preceded the motor dysfunction first detected by the rotarod test at ~36 weeks of age. Hence, TDP-43-mediated pathogenesis is associated with an early induction of astrogliosis/GFAP signals and age-dependent neuroinflammation.

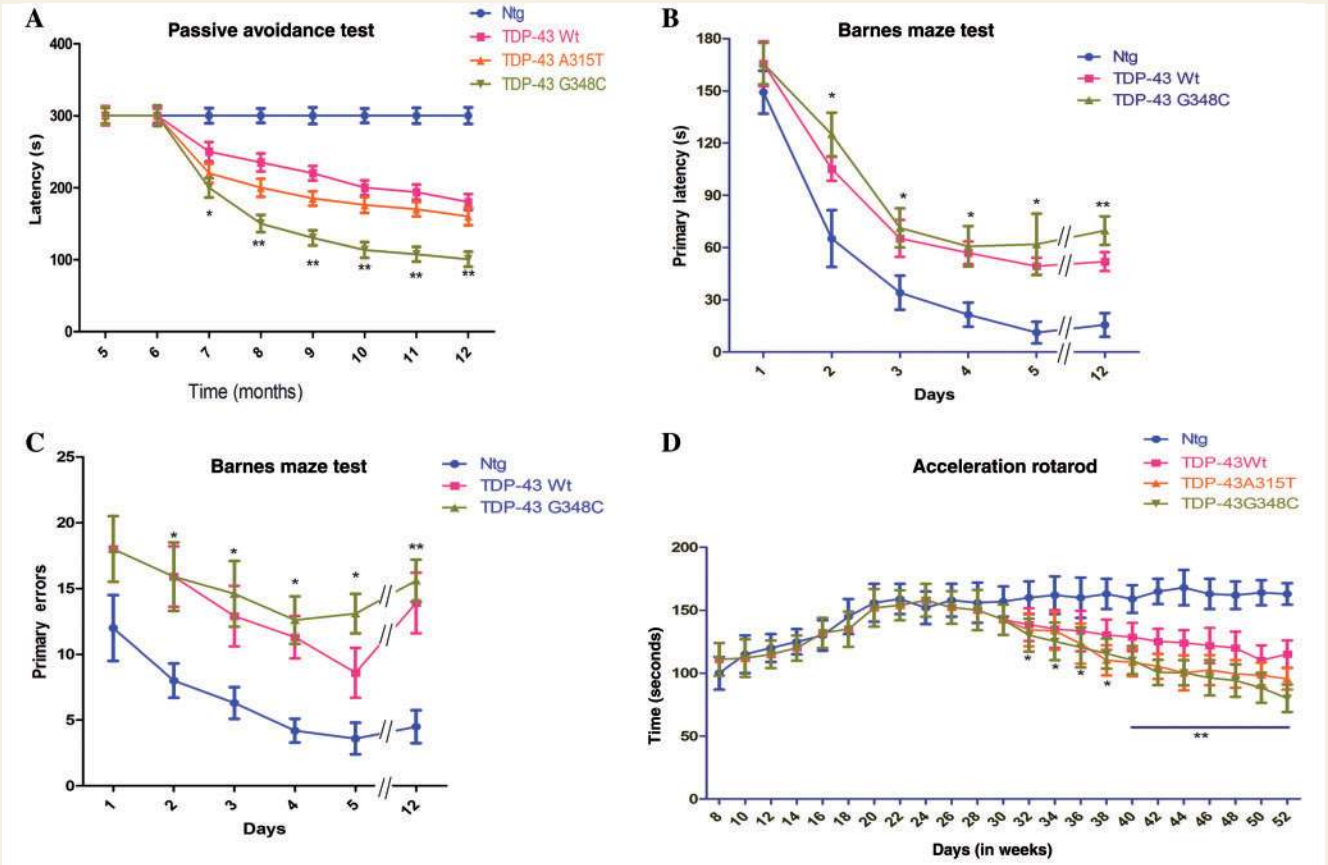

Figure 6 TDP-43 transgenic mice develop cognitive defects and motor dysfunction. (**A**) Passive avoidance test of various transgenic mice was performed every month from 5 to 12 months. Mice were placed in the light chamber, and mice entering in the dark chamber received a small shock. Each test set lasted for 2 days and on the third day, contextual learning/memory of the mice was evaluated based on latency (in s) to enter the dark chamber. A two-way ANOVA with repeated measures was used to study the effect of group (transgenic and non-transgenic mice) and time (in months) on latency to go to the dark chamber. Pairwise comparisons were made using Bonferroni adjustment. TDP-43^{G348C} mice showed significant deficits in contextual learning/memory at 7 months of age ($*P < 0.01$), while TDP-43^{A315T} and wild-type (Wt) TDP-43 mice showed significant deficiencies at 9 months of age ($**P < 0.001$) as compared with non-transgenic controls (Ntg). The cut off time was 300 s; data shown are means ± SEM of 10 different mice from each group. (**B**) Barnes maze test was performed on 10-month-old mice (wild-type TDP-43, TDP-43^{G348C} and non-transgenic). The spatial learning/memory capabilities are expressed as the primary latencies (latency to enter the target quadrant) exhibited in five consecutive sessions and one session at Day 12 of the test for long-term learning/memory analysis. A two-way ANOVA with repeated measures followed by Bonferroni adjustment was used for statistical analysis. TDP-43^{G348C} and to a lesser extent wild-type TDP-43 transgenic mice have severe spatial learning/memory deficits even at Day 2, which became increasingly prominent at Day 5. Long-term memory of TDP-43^{G348C} and wild-type TDP-43 mice are also severely impaired as assessed at Day 12 ($*P < 0.01$, $**P < 0.001$). Results represent means ± SEM of three independent trials ($n = 6$ mice/group). (**C**) The spatial learning/memory capabilities are also expressed as the primary errors (number of errors before entering the target quadrant) exhibited in five consecutive sessions and one session at Day 12 of the test for long-term learning/memory analysis. TDP-43^{G348C} and to a lesser extent wild-type TDP-43 transgenic mice have severe spatial learning/memory deficits even at Day 2, which became increasingly prominent at Day 5. Long-term memory of TDP-43^{G348C} and wild-type TDP-43 mice are also severely impaired as assessed at Day 12 ($*P < 0.01$, $**P < 0.001$). Results represent means ± SEM of three independent trials ($n = 6$ mice/group). (**D**) Accelerating rotarod analysis of mice at various ages from 8 weeks to 52 weeks reveal that TDP-43^{G348C} mice had significant differences in rotarod latencies at 36 weeks of age, TDP-43^{A315T} at 38 weeks and wild-type TDP-43 at 42 weeks of age as compared with non-transgenic control mice. A two-way ANOVA with repeated measures followed by Bonferroni adjustment was used for statistical analysis, $*P < 0.01$, $**P < 0.001$. Data represent means ± SEM of three independent trials ($n = 12$ mice/group).

Discussion

Here we report the generation and characterization of novel transgenic mouse models of amyotrophic lateral sclerosis-FTLD based on expression of genomic fragments encoding wild-type TDP-43 or mutants (A315T and G348C). The mouse models reported here carry TDP-43 transgenes under their own promoters resulting in ubiquitous and moderate expression (~3-fold) of human TDP-43 messenger RNA species. Most of the mouse models of TDP-43 reported previously have shown early paralysis followed by death.

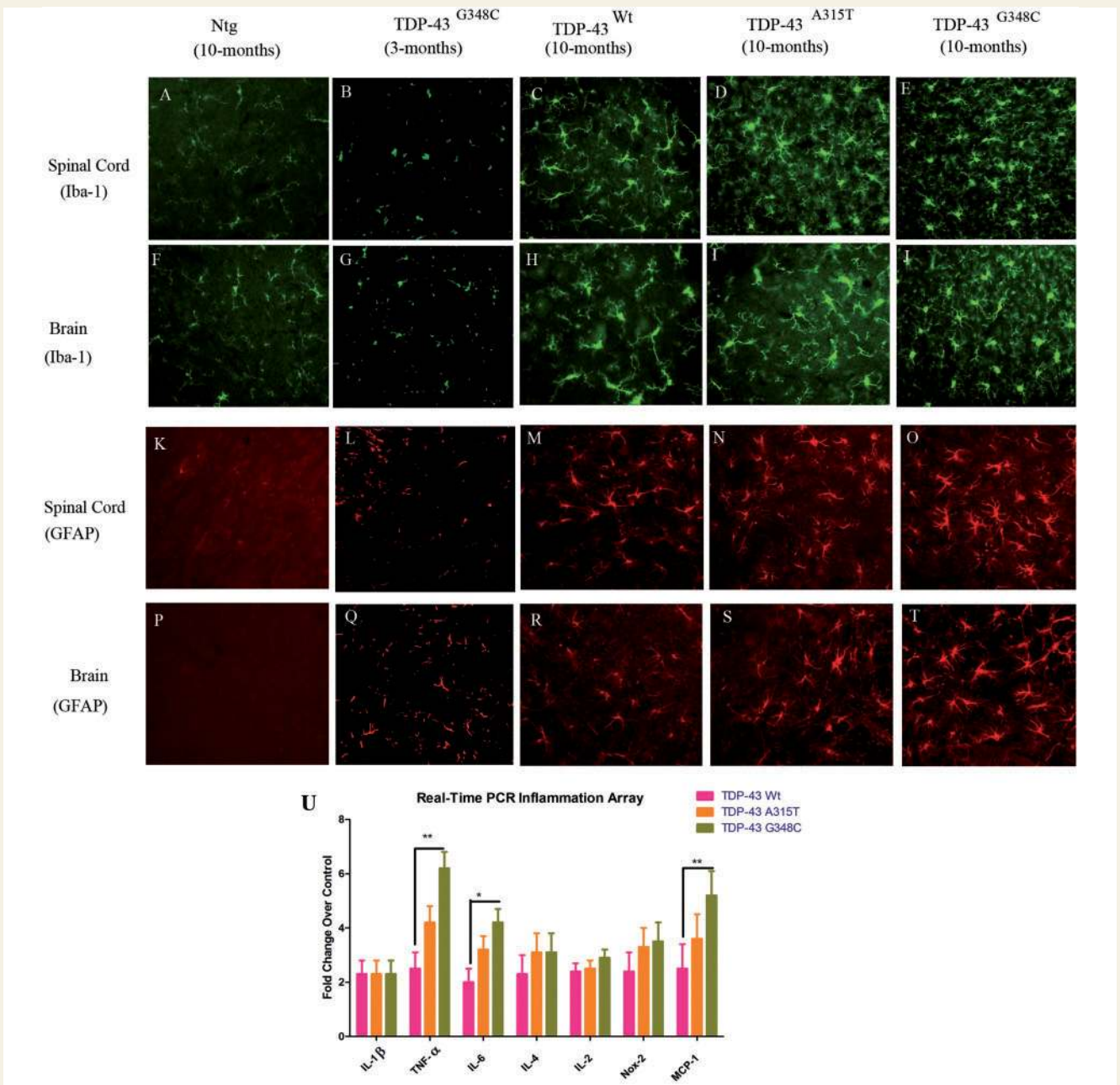

Figure 7 Neuroinflammation in TDP-43 transgenic mice. (**A–H**) Immunofluorescence of the spinal cord (**A–E**) and brain (**F–J**) sections of non-transgenic (Ntg), wild-type (Wt) TDP-43, TDP-43^{A315T} and TDP-43^{G348C} mice was performed using anti-Iba-1 antibody. In the spinal cord, microglial proliferation was abundant in 10-month-old TDP-43^{G348C} mice (**E**), followed by age-matched TDP-43^{A315T} (**D**) and wild-type TDP-43 mice (**C**) as compared with non-transgenic control mice (**A**) and 3-month-old TDP-43^{G348C} mice (**B**). In brain sections also, microgliosis was intense in TDP-43^{G348C} mice (**J**) as well as in age-matched TDP-43^{A315T} (**I**) and wild-type TDP-43 (**H**) as compared with non-transgenic control mice (**F**) and 3-month-old TDP-43^{G348C} mice (**G**). (**K–T**) Immunofluorescence of the spinal cord (**K–O**) and brain (**P–T**) sections of non-transgenic, wild-type TDP-43, TDP-43^{A315T} and TDP-43^{G348C} mice was performed using anti-GFAP antibody. In the spinal cord, astroglial proliferation was abundant in 10-month-old TDP-43^{G348C} mice (**O**), followed by age-matched TDP-43^{A315T} (**N**) and wild-type TDP-43 (**M**) as compared with non-transgenic control mice (**K**) and 3-month-old TDP-43^{G348C} mice (**L**). In brains sections also, microgliosis was abundant in TDP-43^{G348C} mice (**T**) followed by age-matched TDP-43^{A315T} (**S**) and wild-type TDP-43 (**R**) as compared with non-transgenic control mice (**P**) and 3-month-old TDP-43^{G348C} mice (**Q**). (**U**) Quantitative real-time PCR was performed on spinal cord tissue samples from 10-month-old wild-type TDP-43, TDP-43^{A315T} and TDP-43^{G348C} transgenic mice and expressed as fold change over non-transgenic control littermates normalized to Atp-5α levels. One-way ANOVA was used with Tukey's *post hoc* comparison for statistical analysis ($n = 5$ mice/group), $^{*}P < 0.01$, $^{**}P < 0.001$. The levels of tumour necrosis factor-α (TNF-α; 2.7-fold, $^{**}P < 0.001$), interleukin-6 (IL-6; 2-fold, $^{*}P < 0.01$) and monocyte chemotactic protein-1 (MCP-1; 2.5-fold, $^{**}P < 0.001$) were upregulated in TDP-43^{G348C} mice as compared with wild-type TDP-43 mice. Data represent means ± SEM of three independent experiments. Scale bars = 50 μm (**A–T**).

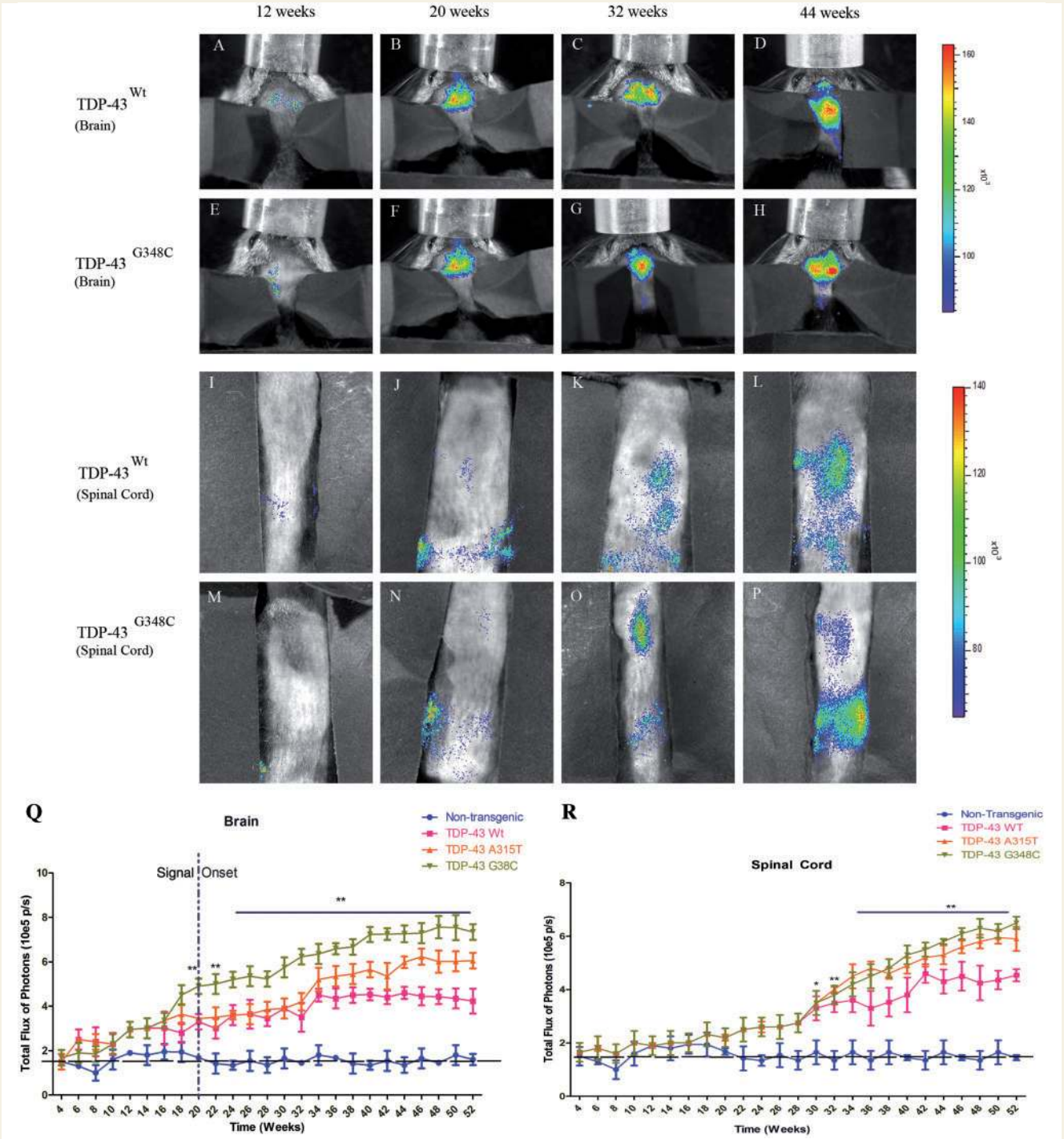

Figure 8 *In vivo* imaging revealed onset of astrocytosis before onset of behavioural impairments in doubly transgenic mice TDP-43/GFAP-luc. (**A–H**) *In vivo* bioluminescence imaging of astrocytes activation was studied at various time points in the brain of GFAP-luc/wild-type TDP-43 (**A–D**) and GFAP-luc/TDP-43^{G348C} (**E–H**) mice. Note that the GFAP-luc/TDP-43^{G348C} (**F**) mice had significant increase of GFAP promoter activity at 5 months (20 weeks) of age compared with GFAP-luc/wild-type TDP-43 (**B**) mice. (**I–P**) Typical sequence of images of the spinal cord area obtained from of GFAP-luc/wild-type TDP-43 (**I–L**) and GFAP-luc/TDP-43^{G348C} (**M–P**) mice at different time points by *in vivo* imaging. Significant GFAP promoter activity can be observed in GFAP-luc/wild-type TDP-43 (**K**) and GFAP-luc/TDP-43^{G348C} (**O**) mice at 8 months (32 weeks) of age. (**Q–R**) Longitudinal quantitative analysis of the total photon GFAP-signal/bioluminescence (total flux of photon/s) in GFAP-luc/wild-type TDP-43, GFAP-luc/TDP-43^{A315T} and GFAP-luc/TDP-43^{G348C} mice in the brain (**Q**) and spinal cord (**R**). A two-way ANOVA with repeated measures followed by Bonferroni adjustment was used for statistical analysis, $*P < 0.01$, $**P < 0.001$. Data represent means ± SEM of three independent experiments ($n = 12$ mice/group).

However, these mouse models are based on high expression levels of TDP-43 transgenes that can mask age-dependent pathogenic pathways. Mice expressing either wild-type or mutant TDP-43 (A315T and M337V) showed aggressive paralysis accompanied by increased ubiquitination (Wegorzewska *et al.*, 2009; Stallings *et al.*, 2010; Wils *et al.*, 2010; Xu *et al.*, 2010), but the lack of ubiquitinated TDP-43-positive inclusions raises concerns about their validity as models of human amyotrophic lateral sclerosis disease. Another concern is the restricted expression of TDP-43 species with the use of Thy1.2 and prion promoters. To better mimic the ubiquitous and moderate levels of TDP-43 occurring in the human context, it seems more appropriate to generate transgenic mice with genomic DNA fragments of TDP-43 gene with its own promoter. As in human neurodegenerative disease, our TDP-43 transgenic mice exhibited age-related phenotypic defects including impairment in contextual learning/memory and spatial learning/memory as determined by the passive avoidance and Barnes maze tests. Long-term memory of 10-month-old TDP-43^{G348C} transgenic mice was severely impaired according to the Barnes maze test. The TDP-43^{G348C}, TDP-43^{A315T} and, to a lesser extent, wild-type TDP-43 mice also exhibited motor deficits as depicted by significant reductions in latency in the accelerating rotarod test.

Cognitive and motor deficits in TDP-43 transgenic mice prompted us to test the underlying pathological and biochemical changes in these mice. Western blot analysis of spinal cord lysates of transgenic mice revealed ~25 kDa and ~35 kDa TDP-43 cleavage fragments that increased in levels with age. Previous studies demonstrated cytotoxicity of the ~25 kDa fragment (Zhang *et al.*, 2009). Immunofluorescence studies with human TDP-43-specific monoclonal antibodies revealed TDP-43 cytoplasmic aggregates in the spinal cord of TDP-43^{G348C}, TDP-43^{A315T} and to a lesser extent in wild-type TDP-43 mice. The cytoplasmic TDP-43-positive inclusions were ubiquitinated. The TDP-43-positive ubiquitinated cytoplasmic inclusions, along with ~25 kDa cytotoxic fragments, are reminiscent of those described in studies on patients with amyotrophic lateral sclerosis and FTLD-U (Neumann *et al.*, 2006). The co-immunoprecipitation of ubiquitin with anti-TDP-43 antibody and inversely of TDP-43 with anti-ubiquitin antibody (Fig. 2U and V) using spinal cord samples from TDP-43^{G348C} mice further confirmed the association of TDP-43 with ubiquitinated protein aggregates. However, TDP-43 itself was not extensively ubiquitinated. A thorough survey of articles on TDP-43 led us to the conclusion that there is no compelling biochemical evidence in literature supporting the general belief that TDP-43 is the major poly-ubiquitinated protein in the TDP-43-positive inclusions. We could find only one blot from one amyotrophic lateral sclerosis case in one paper (Neumann *et al.*, 2006) that revealed a very weak detection of high molecular weight smear with anti-TDP-43 after TDP-43 immunoprecipitation. A subsequent paper (Sanelli *et al.*, 2007) concluded from 3D-deconvolution imaging that TDP-43 is not, in fact, the major ubiquitinated target in ubiquitinated inclusions of amyotrophic lateral sclerosis.

The TDP-43 transgenic mice described here exhibit perikaryal and axonal aggregates of intermediate filaments, another hallmark of degenerating motor neurons in amyotrophic lateral sclerosis (Carpenter, 1968; Corbo and Hays, 1992; Migheli *et al.*, 1993). Before the onset of behavioural changes in these mice, peripherin aggregates form in the spinal cord and brain sections of TDP-43^{G348C} as well as in TDP-43^{A315T} transgenic mice. These peripherin inclusions were also seen in the hippocampal region of the brain of TDP-43^{G348C} mice. Normally, peripherin is not expressed in brain. However, it is known that peripherin expression in the brain can be upregulated after injury or stroke (Beaulieu *et al.*, 2002). The enhanced peripherin levels in these mice are probably due to an upregulation of interleukin-6, a cytokine that can trigger peripherin expression (Sterneck *et al.*, 1996). Sustained peripherin overexpression by >4-fold in transgenic mice was found previously to provoke progressive motor neuron degeneration during aging (Beaulieu *et al.*, 1999). In addition, we detected in TDP-43 transgenic mice the presence of abnormal splicing variants of peripherin, such as Per61, that can contribute to formation of intermediate filament aggregates (Robertson *et al.*, 2003). Using Per61-specific antibodies, we detected peripherin inclusions in the spinal cord sections of TDP-43^{G348C} mice, but not in wild-type TDP-43 mice (Fig. 3). The occurrence of specific splicing peripherin variants has also been reported in human amyotrophic lateral sclerosis cases (Xiao *et al.*, 2008).

In addition, we detected neurofilament protein anomalies in TDP-43^{G348C} mice. Double immunofluorescence revealed the detection of heavy neurofilament protein and medium neurofilament protein in inclusion bodies with peripherin in the spinal cord of TDP-43^{G348C} mice. Moreover, we found that light neurofilament protein is downregulated in the spinal cord lysates of TDP-43^{G348C} mice, a phenomenon that has also been observed in motor neurons of amyotrophic lateral sclerosis cases (Wong *et al.*, 2000). A decrease in light neurofilament protein levels may explain in part the age-related axonal atrophy detected in TDP-43 mice. Previous studies with light neurofilament protein knockout mice demonstrated that such substantial shift in calibres of large myelinated axons provokes a reduction of axon conduction velocity by ~3-fold (Kriz *et al.*, 2000). In large animals with long peripheral nerves, this would cause neurological disease. A loss of neurofilaments due to a homozygous recessive mutation in the *NEFL* gene was found recently to cause a severe early-onset axonal neuropathy (Yum *et al.*, 2009).

Age-related neuroinflammation constitutes another striking feature of the TDP-43 transgenic mice. *In vivo* imaging of biophotonic doubly transgenic mice bearing TDP-43 and GFAP-luc transgenes showed that astrocytes are activated as early as 20 weeks in the brain of GFAP-luc/TDP-43^{G348C} mice followed by activation in the spinal cord at ~30 weeks of age. The signal intensity for astrocytosis in GFAP-luc/TDP-43^{A315T} and GFAP-luc/wild-type TDP-43 was less than in GFAP-luc/TDP-43^{G348C} mice. It is noteworthy that the induction of astrogliosis in the brain and spinal cord in all three TDP-43 mouse models preceded by 6–8 weeks the appearance of cognitive and motor defects. This finding is in line with the recent view of an involvement of reactive astrocytes in amyotrophic lateral sclerosis pathogenesis (Barbeito *et al.*, 2004; Di Giorgio *et al.*, 2007, 2008; Julien, 2007; Nagai *et al.*, 2007).

In conclusion, the TDP-43 transgenic mice described here mimic several aspects of the behavioural, pathological and biochemical features of human amyotrophic lateral sclerosis/FTLD including

age-related development of motor and cognitive dysfunction, cytoplasmic TDP-43-positive ubiquitinated inclusions, intermediate filament abnormalities, axonopathy and neuroinflammation. Why is there no overt degeneration in our TDP-43 mouse models? Unlike previous TDP-43 transgenic mice, these transgenics were made with a genomic fragment that contains 3′ sequence auto-regulating TDP-43 synthesis (Polymenidou *et al*., 2011). So, the TDP-43 levels remain moderate. The ubiquitous TDP-43 ~3-fold overexpression in these mice mimics the ~2.5-fold increase of TDP-43 messenger RNA measured in the spinal cord of human sporadic amyotrophic lateral sclerosis by quantitative real-time PCR (V. Swarup, D. Phaneuf, N. Dupré, S. Petri, M. Strong, J. Kriz and J-P. Julien, unpublished results). In human amyotrophic lateral sclerosis cases carrying TDP-43 mutations, it takes many decades before amyotrophic lateral sclerosis disease onset. The factors that trigger the onset are unknown but perhaps future studies with TDP-43 mouse models might provide some insights. In any case, our new TDP-43 mouse models should provide valuable tools for unravelling pathogenic pathways of amyotrophic lateral sclerosis/FTLD and for preclinical drug testing.

Acknowledgements

We thank Genevieve Soucy for technical assistance. We are grateful to Jean-Nicolas Audet and the transgenic facility of Centre Hospitalier Universitaire de Québec (CHUQ) for generating and maintaining transgenic mice.

Funding

Canadian Institutes of Health Research (CIHR); Amyotrophic lateral sclerosis Society of Canada; Muscular Dystrophy of Canada; Fondation André-Delambre. J.-P.J. holds a Canada Research Chair Tier 1 in mechanisms of neurodegeneration. J.K. holds a R and D/HRF/CIHR Career Award. V.S. is the recipient of the Merit Scholarship for Foreign Students (FQRNT, Quebec, Canada).

Supplementary material

Supplementary material is available at *Brain* online.

References

Barbeito LH, Pehar M, Cassina P, Vargas MR, Peluffo H, Viera L, et al. A role for astrocytes in motor neuron loss in amyotrophic lateral sclerosis. Brain Res Brain Res Rev 2004; 47: 263–74.

Beaulieu JM, Kriz J, Julien JP. Induction of peripherin expression in subsets of brain neurons after lesion injury or cerebral ischemia. Brain Res 2002; 946: 153–61.

Beaulieu JM, Nguyen MD, Julien JP. Late onset of motor neurons in mice overexpressing wild-type peripherin. J Cell Biol 1999; 147: 531–44.

Bose JK, Wang IF, Hung L, Tarn WY, Shen CK. TDP-43 overexpression enhances exon 7 inclusion during the survival of motor neuron pre-mRNA splicing. J Biol Chem 2008; 283: 28852–9.

Buratti E, Dork T, Zuccato E, Pagani F, Romano M, Baralle FE. Nuclear factor TDP-43 and SR proteins promote in vitro and in vivo CFTR exon 9 skipping. EMBO J 2001; 20: 1774–84.

Cairns NJ, Neumann M, Bigio EH, Holm IE, Troost D, Hatanpaa KJ, et al. TDP-43 in familial and sporadic frontotemporal lobar degeneration with ubiquitin inclusions. Am J Pathol 2007; 171: 227–40.

Carpenter S. Proximal axonal enlargement in motor neuron disease. Neurology 1968; 18: 841–51.

Corbo M, Hays AP. Peripherin and neurofilament protein coexist in spinal spheroids of motor neuron disease. J Neuropathol Exp Neurol 1992; 51: 531–7.

Dequen F, Bomont P, Gowing G, Cleveland DW, Julien JP. Modest loss of peripheral axons, muscle atrophy and formation of brain inclusions in mice with targeted deletion of gigaxonin exon 1. J Neurochem 2008; 107: 253–64.

Di Giorgio FP, Boulting GL, Bobrowicz S, Eggan KC. Human embryonic stem cell-derived motor neurons are sensitive to the toxic effect of glial cells carrying an ALS-causing mutation. Cell Stem Cell 2008; 3: 637–48.

Di Giorgio FP, Carrasco MA, Siao MC, Maniatis T, Eggan K. Non-cell autonomous effect of glia on motor neurons in an embryonic stem cell-based ALS model. Nat Neurosci 2007; 10: 608–14.

Forman MS, Trojanowski JQ, Lee VM. TDP-43: a novel neurodegenerative proteinopathy. Curr Opin Neurobiol 2007; 17: 548–55.

Gitcho MA, Baloh RH, Chakraverty S, Mayo K, Norton JB, Levitch D, et al. TDP-43 A315T mutation in familial motor neuron disease. Ann Neurol 2008; 63: 535–8.

Gros-Louis F, Kriz J, Kabashi E, McDearmid J, Millecamps S, Urushitani M, et al. Als2 mRNA splicing variants detected in KO mice rescue severe motor dysfunction phenotype in Als2 knock-down zebrafish. Hum Mol Genet 2008; 17: 2691–702.

Hodges JR, Davies RR, Xuereb JH, Casey B, Broe M, Bak TH, et al. Clinicopathological correlates in frontotemporal dementia. Ann Neurol 2004; 56: 399–406.

Julien JP. ALS: astrocytes move in as deadly neighbors. Nat Neurosci 2007; 10: 535–7.

Kabashi E, Valdmanis PN, Dion P, Spiegelman D, McConkey BJ, Vande Velde C, et al. TARDBP mutations in individuals with sporadic and familial amyotrophic lateral sclerosis. Nat Genet 2008; 40: 572–4.

Keller AF, Gravel M, Kriz J. Live imaging of amyotrophic lateral sclerosis pathogenesis: disease onset is characterized by marked induction of GFAP in Schwann cells. Glia 2009; 57: 1130–42.

Keller AF, Gravel M, Kriz J. Treatment with minocycline after disease onset alters astrocyte reactivity and increases microgliosis in SOD1 mutant mice. Exp Neurol 2010; 228: 69–79.

Kriz J, Meier J, Julien JP, Padjen AL. Altered ionic conductances in axons of transgenic mouse expressing the human neurofilament heavy gene: a mouse model of amyotrophic lateral sclerosis. Exp Neurol 2000; 163: 414–21.

Lagier-Tourenne C, Cleveland DW. Rethinking ALS: the FUS about TDP-43. Cell 2009; 136: 1001–4.

Lomen-Hoerth C, Murphy J, Langmore S, Kramer JH, Olney RK, Miller B. Are amyotrophic lateral sclerosis patients cognitively normal? Neurology 2003; 60: 1094–7.

Lu CH, Kalmar B, Malaspina A, Greensmith L, Petzold A. A method to solubilise protein aggregates for immunoassay quantification which overcomes the neurofilament 'hook' effect. J Neurosci Methods 2011; 195: 143–50.

Mercado PA, Ayala YM, Romano M, Buratti E, Baralle FE. Depletion of TDP 43 overrides the need for exonic and intronic splicing enhancers in the human apoA-II gene. Nucleic Acids Res 2005; 33: 6000–10.

Migheli A, Pezzulo T, Attanasio A, Schiffer D. Peripherin immunoreactive structures in amyotrophic lateral sclerosis. Lab Invest 1993; 68: 185–91.

Nagai M, Re DB, Nagata T, Chalazonitis A, Jessell TM, Wichterle H, Przedborski S. Astrocytes expressing ALS-linked mutated SOD1 release factors selectively toxic to motor neurons. Nat Neurosci 2007; 10: 615–22.

Neumann M, Sampathu DM, Kwong LK, Truax AC, Micsenyi MC, Chou TT, et al. Ubiquitinated TDP-43 in frontotemporal lobar degeneration and amyotrophic lateral sclerosis. Science 2006; 314: 130–3.

Noto YI, Shibuya K, Sato Y, Kanai K, Misawa S, Sawai S, et al. Elevated CSF TDP-43 levels in amyotrophic lateral sclerosis: Specificity, sensitivity, and a possible prognostic value. Amyotroph Lateral Scler 2010.

Ou SH, Wu F, Harrich D, Garcia-Martinez LF, Gaynor RB. Cloning and characterization of a novel cellular protein, TDP-43, that binds to human immunodeficiency virus type 1 TAR DNA sequence motifs. J Virol 1995; 69: 3584–96.

Polymenidou M, Lagier-Tourenne C, Hutt KR, Huelga SC, Moran J, Liang TY, et al. Long pre-mRNA depletion and RNA missplicing contribute to neuronal vulnerability from loss of TDP-43. Nat Neurosci 2011; 14: 459–68.

Prut L, Abramowski D, Krucker T, Levy CL, Roberts AJ, Staufenbiel M, Wiessner C. Aged APP23 mice show a delay in switching to the use of a strategy in the Barnes maze. Behav Brain Res 2007; 179: 107–10.

Robertson J, Doroudchi MM, Nguyen MD, Durham HD, Strong MJ, Shaw G, et al. A neurotoxic peripherin splice variant in a mouse model of ALS. J Cell Biol 2003; 160: 939–49.

Rutherford NJ, Zhang YJ, Baker M, Gass JM, Finch NA, Xu YF, et al. Novel mutations in TARDBP (TDP-43) in patients with familial amyotrophic lateral sclerosis. PLoS Genet 2008; 4: e1000193.

Sanelli T, Xiao S, Horne P, Bilbao J, Zinman L, Robertson J. Evidence that TDP-43 is not the major ubiquitinated target within the pathological inclusions of amyotrophic lateral sclerosis. Journal of neuropathology and experimental neurology 2007; 66: 1147–53.

Seeley WW. Selective functional, regional, and neuronal vulnerability in frontotemporal dementia. Curr Opin Neurol 2008; 21: 701–7.

Sreedharan J, Blair IP, Tripathi VB, Hu X, Vance C, Rogelj B, et al. TDP-43 mutations in familial and sporadic amyotrophic lateral sclerosis. Science 2008; 319: 1668–72.

Stallings NR, Puttaparthi K, Luther CM, Burns DK, Elliott JL. Progressive motor weakness in transgenic mice expressing human TDP-43. Neurobiol Dis 2010; 40: 404–14.

Sterneck E, Kaplan DR, Johnson PF. Interleukin-6 induces expression of peripherin and cooperates with Trk receptor signaling to promote neuronal differentiation in PC12 cells. J Neurochem 1996; 67: 1365–74.

Talbot K, Ansorge O. Recent advances in the genetics of amyotrophic lateral sclerosis and frontotemporal dementia: common pathways in neurodegenerative disease. Hum Mol Genet 2006; 15: R182–7.

Van Deerlin VM, Leverenz JB, Bekris LM, Bird TD, Yuan W, Elman LB, et al. TARDBP mutations in amyotrophic lateral sclerosis with TDP-43 neuropathology: a genetic and histopathological analysis. Lancet Neurol 2008; 7: 409–16.

Wegorzewska I, Bell S, Cairns NJ, Miller TM, Baloh RH. TDP-43 mutant transgenic mice develop features of ALS and frontotemporal lobar degeneration. Proc Natl Acad Sci USA 2009; 106: 18809–14.

Wils H, Kleinberger G, Janssens J, Pereson S, Joris G, Cuijt I, et al. TDP-43 transgenic mice develop spastic paralysis and neuronal inclusions characteristic of ALS and frontotemporal lobar degeneration. Proc Natl Acad Sci USA 2010; 107: 3858–63.

Wong NK, He BP, Strong MJ. Characterization of neuronal intermediate filament protein expression in cervical spinal motor neurons in sporadic amyotrophic lateral sclerosis (ALS). J Neuropathol Exp Neurol 2000; 59: 972–82.

Xiao S, Tjostheim S, Sanelli T, McLean JR, Horne P, Fan Y, et al. An aggregate-inducing peripherin isoform generated through intron retention is upregulated in amyotrophic lateral sclerosis and associated with disease pathology. J Neurosci 2008; 28: 1833–40.

Xu YF, Gendron TF, Zhang YJ, Lin WL, D'Alton S, Sheng H, et al. Wild-type human TDP-43 expression causes TDP-43 phosphorylation, mitochondrial aggregation, motor deficits, and early mortality in transgenic mice. J Neurosci 2010; 30: 10851–9.

Yokoseki A, Shiga A, Tan CF, Tagawa A, Kaneko H, Koyama A, et al. TDP-43 mutation in familial amyotrophic lateral sclerosis. Ann Neurol 2008; 63: 538–42.

Yum SW, Zhang J, Mo K, Li J, Scherer SS. A novel recessive Nefl mutation causes a severe, early-onset axonal neuropathy. Ann Neurol 2009; 66: 759–70.

Zhang YJ, Xu YF, Cook C, Gendron TF, Roettges P, Link CD, et al. Aberrant cleavage of TDP-43 enhances aggregation and cellular toxicity. Proc Natl Acad Sci USA 2009; 106: 7607–12.